HOKKAIDO UNIVERSITY

Title	A numerical solution method for the fractional moment problem within engineering
Author(s)	Wang, Yifan; Tani, Ryuichi; Uchida, Kenetsu
Citation	Engineering Computations, 42(2), 637-666 https://doi.org/10.1108/EC-09-2024-0808
Issue Date	2025-03-04
Doc URL	https://hdl.handle.net/2115/94144
Rights	This author accepted manuscript is deposited under a Creative Commons Attribution Non-commercial 4.0 International (CC BY-NC) licence. This means that anyone may distribute, adapt, and build upon the work for non-commercial purposes, subject to full attribution. If you wish to use this manuscript for commercial purposes, please contact permissions@emerald.com
Rights(URL)	https://creativecommons.org/licenses/by-nc/4.0/
Type	journal article
File Information	manuscript.pdf

Hokkaido University Collection of Scholarly and Academic Papers : HUSCAP

A Numerical Solution Method for the Fractional Moment Problem within Engineering

Abstract

In the field of engineering, the fractional moments of random variables play a crucial role and are widely utilized. They are applied in various areas such as structural reliability assessment and analysis, studying the response characteristics of random vibration systems, and optimizing signal processing and control systems. This study focuses on calculating the fractional moments of positive random variables encountered in engineering. By integrating Laplace transforms with fractional derivatives, both analytical and practical numerical solutions are derived. Furthermore, specific practical application methods are provided. This approach allows for the stable and highly accurate calculation of fractional moments based on the integer moments of random variables. Data experiments included in this study demonstrate the effectiveness of this method in solving fractional moment calculations in engineering. Compared to traditional methods, the proposed method offers significant advantages in stability and accuracy, which can further advance research in the engineering field that employs fractional moments.

Key Words: Fractional moments; Random Variables; Numerical Solution.

1. Introduction

1.1 Background

Fractional moments of random variables are extensively utilized in engineering research, particularly in statistical analysis. In signal processing, fractional moments describe the statistical characteristics of signals with fractal properties and are used in noise analysis to handle noise with long memory or heavy-tailed distributions. In structural engineering, fractional moments often describe the stress-strain relationship of materials for structural reliability analysis, as well as predict the response characteristics of complex structures under random vibrations [1]. In financial engineering, fractional moments describe the heavy-tailed distribution characteristics of financial asset returns, enabling more accurate risk assessment and aiding in the development of precise asset pricing models. In reliability research, fractional moments are widely applied to life prediction and reliability evaluation of systems with complex failure mechanisms [2, 3]. In control engineering, fractional moments contribute to the design of control systems with enhanced robustness against uncertainties. In communication engineering, fractional moments describe the multipath and shadowing effects in channels and are thus essential in wireless communication channel modeling. They also help analyze bit error rate characteristics in various noise environments, optimizing communication system performance. Beyond describing the distribution characteristics of random variables, fractional moments are often combined with the maximum entropy principle for reconstructing the probability density functions of related random variables in engineering. Fractional moments have significant practical advantages: they are more sensitive to heavy-tailed distributions, better characterize long memory properties, adapt flexibly to nonlinear and non-Gaussian statistical characteristics, possess extensive statistical information, and are more stable in the presence of outliers or extreme events. Despite the growing importance of fractional moments in engineering, there remains a need for practical computation methods. Existing methods are often impractical, overly complex, or require excessive computational resources. Therefore, developing a widely

applicable, easy-to-operate, accurate, and stable method for computing fractional moments of random variables is crucial for advancing research and practical applications in signal processing, structural engineering, communication engineering, and other fields.

1.2 Literature Review

There are various methods for calculating the fractional moments of random variables, with some being well-established and widely used. These methods can be classified into three main categories: analytical methods, numerical integration methods, and Monte Carlo simulation methods.

Analytical methods involve using analytical expressions or similar principles to calculate the fractional moments of random variables. Typical approaches include direct derivation of analytical expressions, chaos polynomial expansion, fractional derivative methods, and Taylor expansion methods. Among these, the direct derivation of analytical expressions is the most straightforward. For example, analytical expressions for the fractional moments of lognormal and normal distributions can be directly derived [4, 5]. However, this approach requires prior knowledge of the probability density function of the random variable, and further mathematical derivation is needed. Some probability density functions are too complex to allow for the derivation of analytical expressions for fractional moments. In engineering, the probability density functions of some random variables are unknown, limiting the practical application of this method. The chaos polynomial expansion method is another analytical approach used to calculate both fractional and integer moments of random variables. For instance, Lefebvre [6] proposed a method for calculating high-order integer moments using chaos polynomials, and [7] applied the same principle to fractional moments. Despite its capability, the chaos polynomial method is complex and resource-intensive, making it impractical for engineering applications. Many scholars have derived analytical expressions for fractional moments based on fractional derivatives [8-10]. These expressions are mathematically elegant but are often impractical due to stringent application conditions. The Taylor expansion method is widely used in engineering for calculating fractional moments [11, 12]. This method requires only the integer moments of the random variable and can obtain fractional moments through simple calculations. However, the Taylor expansion method shares the same convergence issues as the generalized Newton polynomial, often requiring a large number of integer moments to achieve convergent and accurate results [12]. This leads to significant computational resource consumption and increased errors in high-order moment calculations, causing fluctuations in research outcomes based on fractional moments and hindering progress.

The numerical integration method is another intuitive and effective way to calculate fractional moments. Once the probability density function of the random variable is known, the moments can be calculated directly through numerical integration, such as the Gaussian-Hermite integration method [13]. The Chebyshev polynomial approximation is also used in some studies [14, 15]. Despite its intuitive nature and conceptual simplicity, the numerical integration method has several limitations in practice. Calculating fractional moments involves non-integer powers, which can lead to numerical instability and accuracy issues, particularly with extreme values or long-tail distributions. This may result in inaccurate calculations or numerical overflow, especially in financial engineering, where fractional moments are used to describe the tail behavior of asset returns [16, 17]. Furthermore, the choice of the integration interval and boundary handling can impact the estimation of fractional moments. This is especially important with small samples, where bias can cause significant errors. For instance, in engineering reliability analysis, data are typically limited and noisy, making it

difficult for numerical integration methods to accurately describe the characteristics of stress and strength distributions [18, 19].

The Monte Carlo simulation method is extensively used in engineering to compute fractional moments of random variables. This is particularly advantageous when accurate probability density functions are not available, but sample data is accessible. The Monte Carlo method proves to be a convenient and effective approach for calculating these moments. In practice, this method involves generating random samples, computing their respective higher-order moments, and then determining the overall higher-order moments of the random variables [20, 21]. Given that Monte Carlo simulations involve sample generation and division, numerous optimization techniques have been developed to enhance the efficiency and accuracy of estimating higher-order moments. For instance, Xu and Dang [22] suggested using latinized partially stratified sampling method to improve the computation of higher-order moments in practical scenarios. Additionally, techniques such as bootstrap and variance reduction techniques are effective in optimizing the performance and precision of Monte Carlo simulations [23-25]. Despite its straightforwardness and simplicity, the Monte Carlo simulation method has inherent limitations. The reliance on a finite number of samples to estimate moments can significantly affect the accuracy of fractional moment calculations due to the effective sample size. When employing bootstrap within Monte Carlo simulations, sample bias might skew the estimation results of fractional moments. This issue is particularly pronounced in small sample sizes, where bias can lead to substantial errors.

Analytical methods, numerical integration, and Monte Carlo simulations can all be used to compute the real-order moments of random variables, including both fractional-order and integer-order moments. However, in practical applications, calculating integer-order moments is simpler and more straightforward than computing fractional-order moments. This simplicity is due to the more straightforward and numerically stable definitions and formulas for integer-order moments, which reduce the risk of numerical overflow and instability. In contrast, fractional-order moments involve non-integer exponents, complicating mathematical processing, especially when handling extreme values or long-tailed distributions, and often resulting in less accurate computations. Additionally, with limited samples, integer-order moment estimates are generally more robust and less affected by sample bias and noise. On the other hand, fractional-order moment estimates are more susceptible to these issues, leading to greater estimation bias. Therefore, it is crucial to develop a method for calculating fractional-order moments based on the integer-order moments of random variables. For instance, the Taylor expansion method could be employed for this purpose, although it also faces challenges related to convergence, accuracy, and stability. The primary aim of this study is to introduce a practical method for calculating fractional-order moments derived from integer-order moments, thereby supporting engineering research that relies on fractional-order moment analysis.

1.3 Objectives and Contents

Assuming that random variables in engineering are predominantly positive, this study introduces a numerical solution method that leverages integer-order moments to compute the corresponding fractional moments of these variables. The proposed method, referred to as the Fractional-Folding Moment Transform (FFMT) method, integrates analytical and numerical solution approaches. Analytical solution expressions are derived using fractional derivatives and Laplace transforms. Based on these analytical expressions, numerical solution expressions that can be applied to practical problems are subsequently derived. The study also explores the characteristics of these numerical solution expressions and provides detailed operational procedures.

The innovation of this study lies in the FFMT method, which derives a novel numerical solution approach for solving fractional moment problems encountered in engineering from the perspective of fractional-order derivatives. This provides a new pathway for the practical calculation of fractional moments. The contribution of this research is reflected in the advantages of the FFMT method compared to traditional methods in practical applications. Unlike the commonly used Taylor expansion method for solving fractional moments in the engineering field, the FFMT method does not face convergence issues during the computation process, offering practical benefits in real-world applications. Furthermore, the FFMT method requires fewer integer-order moments to ensure the accuracy and stability of the results. This feature makes the FFMT method particularly useful in problems that involve extensive fractional moment calculations, as it can significantly save computational resources and improve efficiency, such as in the calculation of traffic assignment problem. Furthermore, in contrast to traditional methods like the Taylor expansion method, the FFMT method is straightforward and easy to implement, with a clear and simple process for determining the involved parameters, thereby ensuring its practical applicability.

Section 2 details the derivation process for both the analytical and numerical solution expressions. Section 3 analyzes the characteristics of the FFMT method formula and presents the operational procedure of the FFMT method. Section 4 validates the feasibility and effectiveness of the FFMT method.

2. Derivation of Formulas

2.1 Analytical Formula

Given any random variable V that may occur in engineering applications, where the value of this random variable is strictly positive, and its corresponding probability density function is denoted as $p(V)$, this paper considers only this univariate probability density function, the Laplace transform of the function $p(V)$ can be obtained as follows:

$$\mathcal{L}\{p(V)\}(s) = \int_0^\infty p(V) \cdot e^{-s \cdot V}(dV) \tag{1}$$

Definition 2.1: For complex numbers with a positive real part, the gamma function is defined via a convergent improper integral [26]:

$$\Gamma(\zeta) = \int_0^\infty t^{\zeta-1} \cdot e^{-t} dt\,, \quad \Re(\zeta) > 0 \tag{2}$$

For every positive integer n, given the fact that $\Gamma(1) = 1,\ \Gamma(n) = (n-1)!$ holds.

Definition 2.2: Given an arbitrary real number z, where $z \in \mathbb{R}$, and a non-integer number λ, where $\lambda \in \mathbb{R}^+$ and $\lambda \notin \mathbb{N}$. Subsequently, by combining the Cauchy formula with the concept of iterative integrals, the corresponding generalized fractional-order integral can be expressed by the following formula [27]:

$$I_z^\lambda f(t) = \frac{1}{\Gamma(\lambda)} \int_z^t (t-\tau)^{\lambda-1} f(\tau) d\tau \tag{3}$$

Definition 2.3: Given an arbitrary real number z, where $z \in \mathbb{R}$, and a non-integer number λ, where $\lambda \in \mathbb{R}^+$ and $\lambda \notin \mathbb{N}$. Let $k = \lceil \lambda \rceil,\ \zeta = k - \lambda,\ k-1 < \lambda < k$. The left Riemann-Liouville (R-L) fractional derivatives ${}_z^{RL}D_t^\lambda f$ of order λ are defined by [28]:

$${}_z^{RL}D_t^\lambda f(t) = D^k\left[I_z^\zeta f(t)\right] = \frac{1}{\Gamma(\zeta)} \frac{d^k}{dt^k} \int_z^t (t-\xi)^{\zeta-1} f(\xi)(d\xi) \tag{4}$$

Setting $z \to -\infty$ and applying the R-L type λ-order derivative to Equation (1), following relationship can be obtained:

$$ {}_{-\infty}^{RL}D_s^{\lambda}\left(\mathcal{L}\{p(V)\}(s)\right) = \int_0^{\infty} p(V) \cdot \left[\frac{1}{\Gamma(\zeta)}\frac{d^k}{ds^k}\int_{-\infty}^{s}(s-\xi)^{\zeta-1}\cdot e^{\xi\cdot V}(d\xi)\right](dV) \tag{5} $$

Definition 2.4: If $f: \mathbb{R}_+ \to \mathbb{R}$, then given an arbitrary real number z, where $z \in \mathbb{R}$, and a non-integer number λ, where $\lambda \in \mathbb{R}^+$ and $\lambda \notin \mathbb{N}$. Let $k = \lceil \lambda \rceil$, $\zeta = k - \lambda$, $k-1 < \lambda < k$. The left Caputo fractional derivatives ${}_z^C D_t^{\lambda} f$ of order λ are defined as:

$$ {}_z^C D_t^{\lambda} f(t) = I_t^{\zeta}\left[\frac{d^k f(t)}{dt^k}\right] = \frac{1}{\Gamma(\zeta)}\int_z^t (t-\xi)^{\zeta-1} f^{(k)}(\xi)(d\xi) \tag{6} $$

Corollary 2.1: Given a non-integer number λ, $\lambda \in \mathbb{R}^+ \,\&\, \lambda \notin \mathbb{N}$, as $z \to -\infty$, the left R-L fractional-order derivative is equivalent to the left Caputo fractional-order derivative, as shown in the following relationship. The specific proof can be found in **Appendix A**.

$$ {}_{-\infty}^{RL}D_t^{\lambda} f(t) = {}_{-\infty}^{C}D_t^{\lambda} f(t) \tag{7} $$

Based on Corollary 2.1, Equation (4) can be further transformed into:

$$ {}_{-\infty}^{RL}D_s^{\lambda}\left(\mathcal{L}\{p(V)\}(s)\right) = \int_0^{\infty} {}_{-\infty}^{C}D_s^{\lambda}\,(e^{s\cdot V})p(V)(dV) \tag{8} $$

Corollary 2.2: Given $f(t) = e^{\varepsilon\cdot t}$, as $z \to -\infty$, $\varepsilon > 0$, then for $\lambda \in \mathbb{C}\,(\Re(\lambda) > 0)$, the following result holds true (the proof process is available in **Appendix B**):

$$ {}_{-\infty}^{C}D_t^{\lambda} e^{\varepsilon\cdot t} = \varepsilon^{\lambda} e^{\varepsilon\cdot t} \tag{9} $$

Applying Corollary 2.1 to Equation (6) and setting $s = 0$, following relationship can be obtained:

$$ \begin{aligned} {}_{-\infty}^{RL}D_s^{\lambda}\left(\mathcal{L}\{p(V)\}(s)\right)|_{s=0} &= \int_0^{\infty} V^{\lambda}\cdot e^{s\cdot V}|_{s=0}\cdot p(V)(dV) \\ &= \int_0^{\infty} V^{\lambda} p(V)(dV) = E\left[(V)^{\lambda}\right] \end{aligned} \tag{10} $$

The relationship presented in Equation (10) represents the analytical solution expression contained within the FFMT method, indicating that the non-integer order moments of can be computed using " ${}_{-\infty}^{RL}D_s^{\lambda}\left(\mathcal{L}\{p(V)\}(s)\right)|_{s=0}$ " for any given random variable. However, the mathematical expression of the left R-L fractional derivatives is not suitable for practical applications. Therefore, this research proceeds to derive a more practical numerical solution expression.

2.2 Numerical Formula

Definition 2.5: Given an arbitrary real number z, where $z \in \mathbb{R}$, and a non-integer number λ, where $\lambda \in \mathbb{R}^+$ and $\lambda \notin \mathbb{N}$. The left Grunwald-Letnikov (G-L) fractional derivatives ${}_z^{GL}D_t^{\lambda} f$ of order λ of a function $f(t)$ is defined by [29]:

$$ \begin{aligned} {}_z^{GL}D_t^{\lambda} f(t) &= \lim_{h\to 0}\frac{1}{h^{\alpha}}\sum_{i=0}^{\infty}(-1)^i\binom{\alpha}{i} f(t-ih) \\ &= \lim_{\substack{h\to 0 \\ n=\frac{t-z}{h}}}\frac{1}{h^{\alpha}}\sum_{i=0}^{n}(-1)^i\binom{\alpha}{i} f(t-ih) \end{aligned} \tag{10} $$

Corollary 2.3: Given the assumption that the function $f(t)$ possesses a continuous derivative of order $m+1$, the G-L fractional derivative is congruent to the R-L fractional derivative, as shown below (the proof process is available in **Appendix C**):

$$ {}_{z}^{GL}D_{t}^{\lambda} f(t) = {}_{z}^{RL}D_{t}^{\lambda} f(t) \tag{11} $$

Remark 2.1: For $t \gg z$, from the expression for the coefficients in the G-L fractional derivative, that for large t the role of the history of the behavior of the function $f(t)$ near the lower terminal can be neglected. This results in the establishment of the "short memory principle", indicate that the operator ${}_{z}^{GL}D_{t}^{\lambda}$ only necessitates considering the behavior of $f(t)$ within the recent past.

Defined within the interval $[t-L, t]$, where L represents the memory length, the "short memory principle" can be articulated as follows:

$$ {}_{-\infty}^{GL}D_{t}^{\lambda} f(t) \approx {}_{t-L}^{GL}D_{t}^{\lambda} f(t) \tag{12} $$

Based on the Definition 2.5, Corollary 2.3 and Remark 2.1, the following relationship can be derived:

$$ \begin{aligned} {}_{-\infty}^{RL}D_{s}^{\lambda}\left(\mathcal{L}\{p(V)\}(s)\right)|_{s=0} &= {}_{-\infty}^{GL}D_{s}^{\lambda}\left(\mathcal{L}\{p(V)\}(s)\right)|_{s=0} \\ \approx {}_{s-L}^{GL}D_{s}^{\lambda}\left(\mathcal{L}\{p(V)\}(s)\right)|_{s=0} &= \frac{1}{h^{\alpha}}\sum_{i}^{N}(-1)^{i}\cdot\binom{\alpha}{i}\cdot\left(\mathcal{L}\{p(V)\}(s-ih)\right)|_{s=0} \\ &= E\left[(V)^{\lambda}\right] \end{aligned} \tag{13} $$

In this case, Equation (13) still contains $\left(\mathcal{L}\{p(V)\}(s-ih)\right)$, which remains unsuitable for practical applications. Through further derivation, a numerical solution expression suitable for practical applications is obtained, as stated in the following corollary.

Corollary 2.4: For the random variable V, assuming arbitrary random distributions, the values of non-integer order moments $E\left[(V)^{\lambda}\right]$ can be obtained through the following numerical solution expression (the proof process is available in **Appendix D**):

$$ E\left[(V)^{\lambda}\right] = \sum_{j=0}^{N}\frac{(-1)^{N-j}\cdot(\lambda-N)}{\lambda-j}\cdot\binom{\lambda}{N}\cdot\binom{N}{j}\cdot h^{j-\lambda}\cdot E\left[(V)^{j}\right] \tag{14} $$

where $N = \left\lfloor\frac{L}{h}\right\rfloor$, and L is the memory length, and $\binom{\lambda}{i} = \frac{\lambda\cdot(\lambda-1)\cdot(\lambda-2)\ldots(\lambda-i+1)}{i!} = \frac{\Gamma(\lambda+1)}{\Gamma(\lambda+1-i)i!}$.

The equation in Corollary 2.4 is the core formula of the FFMT method, indicating for random link flow, regardless of the distribution, obtaining its corresponding integer-order moment enables the calculation of the corresponding non-integer order moments by Equation (14).

2.3 Error expression of Numerical formula

The parameter N in the numerical solution expression is highly worthy of elucidation, as it holds significant intrinsic meaning. According to the definition, N adheres to the following relationship:

$$ N = \left\lfloor\frac{L}{h}\right\rfloor \tag{15} $$

where h represents the step length, provided directly with a requirement of h being sufficiently small. Another critical parameter is L, representing the memory length. The value of L plays a crucial role in determining the error size associated with the left Grunwald-Letnikov fractional derivatives method. In essence, this method incurs some inaccuracy as a penalty; hence, the value of L should be selected cautiously to ensure the error remains within the specified range.

Corollary 2.5: Given $|f(t)| \le M$, $a + L < b$, L is the memory length. Given a required accuracy ε, ε can impose a direct impact on the memory length, if $\Delta(t) \le \varepsilon$, then ε further determine the memory length L (the proof process is available in **Appendix E**):

$$ L \ge \left(\frac{M}{\varepsilon\,|\Gamma(1-\lambda)|}\right)^{\frac{1}{\lambda}} \tag{16} $$

Thus far, this part has elucidated and derived the analytical solution expression for arbitrary-order moments utilizing R-L fractional derivatives and Laplace transform. Simultaneously, based on this computational principle and employing G-L fractional derivatives, numerical solution expression for computing arbitrary-order moments of random variables has been proposed, along with the corresponding calculation formulas.

3. Application of Formula

For convenience, the formula in Corollary 2.4 is represented using the following functional expression:

$$f_{N,h}(\lambda, V) = \sum_{j=0}^{N} \frac{(-1)^{N-j} \cdot (\lambda - N)}{\lambda - j} \cdot \binom{\lambda}{N} \cdot \binom{N}{j} \cdot E\left[(V)^j\right] \cdot h^{j-\lambda} \tag{17}$$

In the practical application of the function $f_{N,h}(\lambda, V)$ to calculate the corresponding $E\left[(V)^\lambda\right]$, the values of random variable V and fractional order λ are given and are considered as independent variables of the function $f_{N,h}(\cdot)$. Consequently, the function's output is the corresponding dependent variable. To obtain the result of $E\left[(V)^\lambda\right]$ once the values of the independent variables V and λ are established, there are two corresponding parameters in function $f_{N,h}(\cdot)$ that need to be determined: N and h. Corollary 2.4 provides a numerical solution expression, which inherently contains some error. According to the short memory principle, the memory length L significantly impacts the error magnitude of the numerical solution expression, and the memory length L is directly related to the parameters N and h. Therefore, the values of the parameters N and h in function $f_{N,h}(\cdot)$ will significantly affect the accuracy of the computational results. Once V and λ in function $f_{N,h}(\cdot)$ are determined, there exist specific corresponding values of N and h that minimize the numerical solution error. The parameter N represents the number of integer-order moments used. Essentially, Corollary 2.4 can be understood as linearly combining these N integer-order moments in appropriate proportions to obtain the desired computational result. This appropriate proportion can be represented by h.

3.1 Parameter N

The determination of the parameter N is directly related to the independent variable λ in the function $f_{N,h}(\cdot)$. Using a finite number of integer-order moments to achieve accurate computational results can effectively save computational resources. When the number of integer-order moments exceeds λ, it includes sufficient information from the integer-order moments to obtain sufficiently accurate λ-order moments. Therefore, the optimal strategy for determining the value of N is to set N as the smallest integer greater than λ. Based on this, when λ varies within the corresponding integer interval, denoted as $(i, i+1)$ and $i = \lfloor \lambda \rfloor$, the value of N remains unchanged. Similarly, even if the independent variable V in function $f_{N,h}(\cdot)$ changes, it will not affect the value of N. The equation for N is as follows:

$$N = \lceil \lambda \rceil \tag{18}$$

3.2 Parameter h

Once the values of the independent variables V and λ for the function $f_{N,h}(\cdot)$ are determined, the corresponding value of the parameter N can be identified. At this point, there is an optimal value for the parameter h that minimizes the result error in the function $f_{N,h}(\cdot)$. The FFMT method essentially involves linearly combining N integer-order moments in appropriate proportions to obtain the desired fractional-order moment. When the independent variable V of the function

$f_{N,h}(\cdot)$ remains constant, and the fractional order λ varies within the integer interval $(i, i+1)$, the integer-order moments used for linear combination stay the same. Using the same optimal h value in this scenario ensures a stable and sufficiently accurate result. However, if the independent variable V of function $f_{N,h}(\cdot)$ changes, even if λ remains unchanged, the integer-order moments used for the linear combination will change significantly. In this case, using the same optimal h value will not ensure minimal error, indicating a change in the optimal h value. Thus, when the independent variable V of function $f_{N,h}(\cdot)$ changes, the optimal value of the parameter h also changes. Similarly, when the fractional order λ crosses its corresponding integer interval $(i, i+1)$, the optimal value of the parameter h changes.

Considering that the only known conditions are the values of the integer-order moments of the corresponding random variables, the method to determine the optimal parameter h will only rely on these integer-order moments. Let P be a very small constant. Then set λ' equals to $i + P$. When the difference between the value of function $f_{N,h}(\lambda', V)$ and the value of $E[(V)^i]$ is minimized, the corresponding h value must be optimal, minimizing the computational error of function $f_{N,h}(\cdot)$. Given a new function $g_{\lambda',V}(h)$, as shown below, representing the difference between function $f_{N,h}(\lambda', V)$ and the corresponding $E[(V)^i]$, with h as the independent variable. To find the optimal parameter h, it is necessary to identify the value of h that corresponds to the minimum of function $g_{\lambda',V}(\cdot)$.

$$g_{\lambda',V}(h) = \sum_{j=0}^{N} \frac{(-1)^{N-j} \cdot (\lambda' - N)}{\lambda' - j} \cdot \binom{\lambda'}{N} \cdot \binom{N}{j} \cdot E\left[(V)^j\right] \cdot h^{j-\lambda'} - E\left[(V)^i\right] \tag{19}$$

3.2.1 Existence and Uniqueness of h

Before using function $g_{\lambda',V}(\cdot)$ to determine the optimal h value, it is essential to prove the existence and uniqueness of the minimum in function $g_{\lambda',V}(\cdot)$. When the value of N is either odd or even, it corresponds to different patterns. Therefore, when discussing the characteristics of function $g_{\lambda',V}(h)$, N will be classified and discussed based on its parity.

(1) N is Odd

A new function $G_{\lambda',V}(h)$ is defined, with h serving as the independent variable. The first derivative of function $G_{\lambda',V}(h)$ with respect to h is denoted as function $g_{\lambda',V}(h)$. And C represents an arbitrary constant. The expression for function $G_{\lambda',V}(h)$ is formulated as follows:

$$G_{\lambda',V}(h) = \sum_{j=0}^{N} \frac{(-1)^{N-j} \cdot (\lambda' - N)}{(\lambda' - j) \cdot (j - \lambda' + 1)} \cdot \binom{\lambda'}{N} \cdot \binom{N}{j} \cdot \left[(V)^j\right] \cdot h^{j-\lambda'+1} - E\left[(V)^i\right] \cdot h + C \tag{20}$$

For simplicity, let $\alpha_j = \frac{(-1)^{N-j} \cdot (\lambda' - N)}{(\lambda' - j) \cdot (j - \lambda' + 1)} \cdot \binom{\lambda'}{N} \cdot \binom{N}{j} \cdot \left[(V)^j\right]$ and $\mathcal{T}_j(h) = h^{j-\lambda'+1}$. In this case, function $G_{\lambda',V}(h)$ can be expressed as:

$$G_{\lambda',V}(h) = (\alpha_0 \cdot \mathcal{T}_0 + \alpha_1 \cdot \mathcal{T}_1 + \cdots + \alpha_{N-2} \cdot \mathcal{T}_{N-2}) + \left(\alpha_{N-1} \cdot \mathcal{T}_{N-1} + \alpha_N \cdot \mathcal{T}_N - E\left[(V)^i\right] \cdot h\right) + C \tag{21}$$

As h approaches 0, with $\mathcal{T}_0$ being the highest-order term and $\alpha_0 < 0$, it can be inferred the limit of function $G_{\lambda',V}(h)$:

$$\lim_{h \to 0} G_{\lambda',V}(h) = -\infty \tag{22}$$

Considering the random variable V, which has a range of $(0,+\infty)$ and corresponds to the probability density function $p(V)$, then the validity of relationship $\frac{V^N}{N}-d\left(\frac{V^N}{N}\right)>0$ implies the derivation of the following relationship:

$$\frac{V^N}{N}-d\left(\frac{V^N}{N}\right)>0\Rightarrow\left|\frac{V^{N+1}}{N+1}-V^N\right|_0^{+\infty}>0$$

$$\Rightarrow\int_0^{+\infty}(V^N-N\cdot V^{N-1})dV>0\Rightarrow\int_0^{+\infty}V^N\cdot p(V)dV-\int_0^{+\infty}N\cdot V^{N-1}\cdot p(V)dV>0$$

$$\Rightarrow E[(V)^N]-N\cdot E[(V)^{N-1}]>0 \tag{23}$$

Relaxing specific coefficients, the given relationship still holds true:

$$E[(V)^N]-N\cdot E[(V)^{N-1}]>0\Rightarrow(N-j)\cdot E\left[(V)^{j+1}\right]-(j+1)\cdot E\left[(V)^j\right]>0$$

$$\Rightarrow\frac{(j+1)!\cdot(N-j-1)!\cdot E\left[(V)^j\right]}{j!\cdot(N-j)!\cdot E[(V)^{j+1}]}<1\Rightarrow\frac{(\lambda'-j-2)\cdot(j+1)!\cdot(N-j-1)!\cdot E\left[(V)^j\right]}{(\lambda'-j)\cdot j!\cdot(N-j)!\cdot E[(V)^{j+1}]}<1$$

$$\Rightarrow\frac{\frac{N-\lambda'}{(\lambda'-j)\cdot(\lambda'-j-1)}\cdot\binom{\lambda'}{N}\cdot\binom{N}{j}\cdot E\left[(V)^j\right]}{\frac{N-\lambda'}{(\lambda'-j-1)\cdot(\lambda'-j-2)}\cdot\binom{\lambda'}{N}\cdot\binom{N}{j+1}\cdot E[(V)^{j+1}]}<1 \tag{24}$$

Now considering j ranges from 0 to $N-2$, based on the structural formula of α_j, it is evident that α_j is negative when j is even and positive when j is odd. Assuming j is even, and the range of h is $(0,1]$ in conjunction with Equation (24), the following relationship can be derived:

$$\frac{\alpha_j}{\alpha_{j+1}}>-1\Rightarrow\frac{d(\alpha_{j+1}\cdot\mathcal{T}_{j+1}(h))}{dh}\Big/\frac{d(-\alpha_j\cdot\mathcal{T}_j(h))}{dh}<1 \tag{25}$$

Then considering the remaining terms in function $G_{\lambda',V}(h)$, denoted by function $\mathcal{S}_{\lambda',V}(h)$, excluding C, it can be represented as follows:

$$\mathcal{S}_{\lambda',V}(h)=\alpha_{N-1}\cdot h^{N-\lambda'}+\alpha_N\cdot h^{N-\lambda'+1}-E[(V)^{N-1}]\cdot h \tag{26}$$

Given the very small value of P, function $\mathcal{S}_{\lambda',V}(h)$ can be approximated as an upward-opening quadratic function, where $\mathcal{S}_{\lambda',V}(0)=0$, and its minimum value is negative which located at $h=\frac{E[(V)^{N-1}]-\alpha_{N-1}}{2\cdot\alpha_N}$. Then the following relationship can be derived:

$$\left(\alpha_0\cdot\left(\frac{E[(V)^{N-1}]-\alpha_{N-1}}{2\cdot\alpha_N}\right)^{-\lambda'+1}-\lim_{h\to0}G_{\lambda',V}(h)\right)$$

$$-\left(\begin{array}{c}\alpha_{N-1}\cdot\left(\frac{E[(V)^{N-1}]-\alpha_{N-1}}{2\cdot\alpha_N}\right)^{N-\lambda'}+\alpha_N\cdot\left(\frac{E[(V)^{N-1}]-\alpha_{N-1}}{2\cdot\alpha_N}\right)^{N-\lambda'+1}\\ -E[(V)^{N-1}]\cdot\frac{E[(V)^{N-1}]-\alpha_{N-1}}{2\cdot\alpha_N}\end{array}\right)>0 \tag{27}$$

Based on Equations (25) and (27), for the function $G_{\lambda',V}(\cdot)$, when N is odd, within the range of $(0,1]$, it is impossible to find two distinct values of h $(h_1\neq h_2)$ such that $G_{\lambda',V}(h_1)=G_{\lambda',V}(h_2)$. Therefore, according to the Rolle's lemma, it can be concluded that there are no zeros of the function $g_{\lambda',V}(h)$ within the range $(0,1]$.

Then for simplicity, let $\mathcal{K}_j = \frac{(-1)^{N-j}\cdot(\lambda'-N)}{\lambda'-j}\cdot\binom{\lambda'}{N}\cdot\binom{N}{j}\cdot E\left[(V)^j\right]$, and $\mathcal{U}_j(h) = h^{j-\lambda'}$. Then function $g_{\lambda',V}(h)$ can be expressed as:

$$g_{\lambda',V}(h) = \mathcal{K}_0\cdot\mathcal{U}_0 + \mathcal{K}_1\cdot\mathcal{U}_1 + \cdots + \mathcal{K}_N\cdot\mathcal{U}_N \tag{28}$$

In this case, for the function $g_{\lambda',V}(h)$, as h approaches 0, the highest-order term corresponds to $\mathcal{U}_0$. Considering the parity of N, it can be deduced that $\mathcal{K}_0$ is greater than 0 in this scenario. Therefore, the limit of function $g_{\lambda',V}(h)$ can be derived as follows:

$$\lim_{h\to 0} g_{\lambda',V}(h) = +\infty \tag{29}$$

At this juncture, within the range of $(0,1]$, it has been proved that the function $g_{\lambda',V}(h)$ does not have any zeros. Consequently, it can be inferred that the value of the function $g_{\lambda',V}(h)$ at $h=1$ is greater than 0, i.e., $g_{\lambda',V}(1) > 0$. To further ascertain the characteristics of the function $g_{\lambda',V}(h)$, the first derivative of function $g_{\lambda',V}(h)$ is provided as follows:

$$g^{(1)}_{\lambda',V}(h) = \sum_{j=0}^{N}(-1)^{N-j}\cdot(N-\lambda')\cdot\binom{\lambda'}{N}\cdot\binom{N}{j}\cdot E\left[(V)^j\right]\cdot h^{j-\lambda'-1} \tag{30}$$

For the sake of simplicity, let $\mathcal{I}_j = (-1)^{N-j}(N-\lambda')\binom{\lambda'}{N}\binom{N}{j}E\left[(V)^j\right]$, and $\mathcal{C}_j(h) = h^{j-\lambda'-1}$.

Then function $g^{(1)}_{\lambda',V}(h)$ can be expressed as:

$$g^{(1)}_{\lambda',V}(h) = \mathcal{I}_0\cdot\mathcal{C}_0 + \mathcal{I}_1\cdot\mathcal{C}_1 + \cdots + \mathcal{I}_N\cdot\mathcal{C}_N \tag{31}$$

Following the same principles of computation as with $\lim_{h\to 0} G_{\lambda',V}(h)$, and considering that the value of $\mathcal{I}_0$ is negative, the limit of function $g^{(1)}_{\lambda',V}(h)$ as h approaches 0 is: $\lim_{h\to 0} g^{(1)}_{\lambda',V}(h) = -\infty$. Considering j within the range $[0,N]$, assuming j is even, $\mathcal{I}_j$ is always negative, and $\mathcal{I}_{j+1}$ is always positive. Then the conclusion from Equation (23) can be used to derive the following relationship:

$$\begin{gathered}
E[(V)^N] - N\cdot E[(V)^{N-1}] > 0 \Rightarrow (N-j)\cdot E\left[(V)^{j+1}\right] - (j+1)\cdot E\left[(V)^j\right] > 0 \\
\Rightarrow \frac{(j+1)!\cdot(N-j-1)!\cdot E\left[(V)^j\right]}{j!\cdot(N-j)!\cdot E[(V)^{j+1}]} < 1 \Rightarrow \frac{(j+1)!\cdot(N-j-1)!\cdot E\left[(V)^j\right]}{j!\cdot(N-j)!\cdot E[(V)^{j+1}]} < 1 \\
\Rightarrow \frac{(N-\lambda')\cdot\binom{\lambda'}{N}\cdot\binom{N}{j}\cdot E\left[(V)^j\right]}{(N-\lambda')\cdot\binom{\lambda'}{N}\cdot\binom{N}{j+1}\cdot E[(V)^{j+1}]} < 1 \\
\Rightarrow \frac{\mathcal{I}_j}{\mathcal{I}_{j+1}} > -1
\end{gathered} \tag{32}$$

According to the result of Equation (32), it is evident that the value of the function $g^{(1)}_{\lambda',V}(h)$ at $h=1$ is greater than 0, i.e., $g^{(1)}_{\lambda',V}(1) > 0$. According to the Bolzano-Cauchy theorem, it can be deduced that within the range $(0,1)$, there must exist at least one value of h for which the function

$g^{(1)}_{\lambda',V}(h)$ equals 0. Building upon the conclusion of Equation (32) and incorporating the characteristics of $\mathcal{C}_j$, the following relationship can be further derived:

$$\frac{\mathcal{I}_j}{\mathcal{I}_{j+1}} > -1 \Rightarrow 0 < \frac{d\left(\mathcal{I}_{j+1}\cdot\mathcal{C}_{j+1}(h)\right)}{dh} \Big/ \frac{d(-\mathcal{I}_j\cdot\mathcal{C}_j(h))}{dh} < 1 \tag{33}$$

Then it is evident that the function $g^{(1)}_{\lambda',V}(h)$ has only one zero within the interval $(0,1]$. Continuing to utilize the results of Equation (32) and incorporating the characteristics of $\mathcal{C}_j(h)$, given that the range of j is $[0,N]$, with N being an even number, and for h in the range of $(1,+\infty)$, the following relationship can be derived:

$$0 > \frac{\mathcal{I}_j\cdot\mathcal{C}_j(h)}{\mathcal{I}_{j+1}\cdot\mathcal{C}_{j+1}(h)} > -1 \tag{34}$$

Based on the results of Equation (34), it is evident that within the range of h within $(1,+\infty)$, the value of the function $g^{(1)}_{\lambda',V}(h)$ is always greater than 0. Thus, it has been demonstrated that the shape of the function $g_{\lambda',V}(h)$ approximately resembles an upward-opening quadratic function. The function $g_{\lambda',V}(h)$ necessarily has a single minimum within the range $h\in(0,+\infty)$, and the corresponding value of h that yields this minimum is certainly located within the range $(0,1)$. Consequently, this also indicates that for the formula in Corollary 2.4, when N is an odd number, there exists an optimal value of h that minimizes the corresponding computational error, as shown in the Figure 1.

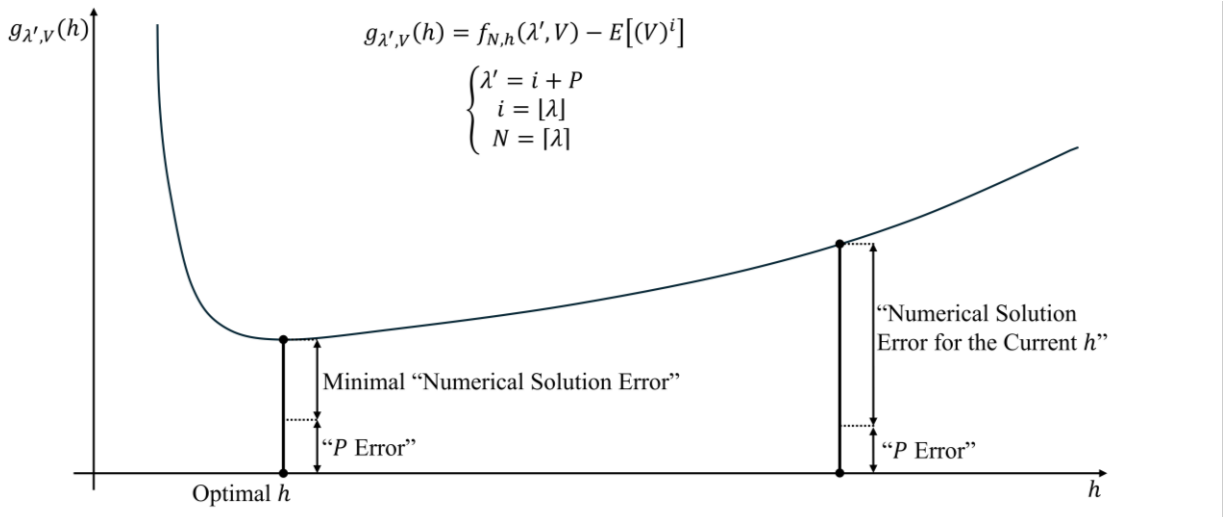

Fig 1. The Approximate Shape of Function $g_{\lambda',V}(h)$ and the Corresponding Sources of Computational Error if N is Odd.

As shown in Figure 1, the value of function $g_{\lambda',V}(h)$ represents the corresponding computational error. It is evident that there will always be a computational error regardless of the value of h, but the magnitude of this error will vary with changes in h. This study assumes that the computational error itself consists of two parts: P error and numerical solution error. Although the value of P used in variable λ' for function $g_{\lambda',V}(h)$ is very small, it is never zero. Therefore, even if the formula in Corollary 2.4 yields a totally accurate result, the value of function $g_{\lambda',V}(h)$ will not

be zero after using λ', but greater than zero. This part of the computational error is caused by P, which is referred to as P error. P error is solely related to the value of P and represents the difference between $E[(V)^{i+P}]$ and $E[(V)^i]$ when applying function $g_{\lambda',V}(h)$. It is an objective error that is independent of the values of N and h. In contrast, the other part of the computational error represented by function $g_{\lambda',V}(h)$ is the numerical solution error. This error originates from the formula in Corollary 2.4 itself, as the formula in Corollary 2.4 is a numerical solution expression and inherently has computational errors. This part of the error is referred to as the numerical solution error. Based on the previous analysis, it has been established that when λ and N are determined, the magnitude of the numerical solution error is related to the value of h, so there exists an optimal h value that minimizes the current numerical solution error. The purpose and significance of finding the optimal h value lie in this context, which is to minimize the numerical solution error component of the computational error represented by the function $g_{\lambda',V}(h)$. The optimal h value corresponds to the h value at which function $g^{(1)}_{\lambda',V}(h)$ equals zero. Therefore, when calculating the optimal h value for odd N, it is only necessary to determine the h value corresponding to $g^{(1)}_{\lambda',V}(h) = 0$. This corresponds to the following relationship:

$$g^{(1)}_{\lambda',V}(h) = 0$$

$$\Rightarrow \sum_{j=0}^{N} (-1)^{N-j} \cdot (N-\lambda') \cdot \binom{\lambda'}{N} \cdot \binom{N}{j} \cdot E\left[(V)^j\right] \cdot h^{j-\lambda'-1} = 0$$

$$\Rightarrow \sum_{j=0}^{N} \frac{(-1)^{N-j} \cdot E\left[(V)^j\right]}{j! \cdot (N-j)!} \cdot h^j = 0 \tag{35}$$

From the result of Equation (35), it is evident that the optimal h value is independent of P. When the values of V and N corresponding to function $g_{\lambda',V}(h)$ remain unchanged, the optimal h value is fixed regardless of the initial value of P. This in turn implies that the role of the current optimal h value is to minimize the numerical solution error, thereby maximizing computational accuracy of FFMT method, and it does not affect the P error. Moreover, the fact that the optimal value of h is independent of P indicates that once the optimal value of h is determined using λ', the corresponding integer-order moments for linear combination remain unchanged even if P varies within the range $(0,1)$. Consequently, even if λ varies within the respective integer interval $(i, i+1)$, the same optimal value of h ensures that the error in the FFMT results remains stable and relatively low.

(2) N is Even

When N is even, based on the function $g_{\lambda',V}(h)$, assuming j is within the range $[0, N-1]$, combining with the result of Equation (24), the following relationship can be obtained when h is within the range $(0,1]$:

$$0 < \frac{d\left(\mathcal{K}_{j+1} \cdot \mathcal{U}_{j+1}(h)\right)}{dh} \Big/ \frac{d(-\mathcal{K}_j \cdot \mathcal{U}_j(h))}{dh} < 1 \tag{36}$$

Similarly, for the function $g_{\lambda',V}(h)$, within the range of j from $[0, N-1]$, when the independent variable h ranges from $(1, +\infty)$, the following relationship can be derived:

$$-1 < \frac{\mathcal{K}_j \cdot \mathcal{U}_j(h)}{\mathcal{K}_{j+1} \cdot \mathcal{U}_{j+1}(h)} < 0 \tag{37}$$

Then, for the remaining terms of the function $g_{\lambda',V}(h)$, with the independent variable h ranges from $(0, +\infty)$, the following relationship can be derived:

$$\frac{d(\mathcal{K}_N \cdot \mathcal{U}_N(h) - E[(V)^{N-1}])}{dh} > 0 \tag{38}$$

Based on the above conclusions, it can be determined that when N is even, the function $g_{\lambda',V}(h)$ is always increasing over the interval $(0, +\infty)$. On the other hand, considering the limits of the function $g_{\lambda',V}(h)$, dented as $\lim_{h\to 0} g_{\lambda',V}(h) = -\infty$ and $\lim_{h\to+\infty} g_{\lambda',V}(h) = +\infty$, within the range $(0, +\infty)$, there must exist a value of h such that $g_{\lambda',V}(h) = 0$. This zero-point h must satisfy the following relationship:

$$g_{\lambda',V}(h) = 0$$
$$\Rightarrow \sum_{j=0}^{N} \frac{(-1)^{N-j} \cdot ((i+P)' - N)}{(i+P)' - j} \cdot \binom{(i+P)'}{N} \cdot \binom{N}{j} \cdot E\left[(V)^j\right] \cdot h^{j-(i+P)'} = E\left[(V)^i\right] \tag{39}$$

For Equation (39), regardless of whether the corresponding h value can be obtained, it is evident that the h value is significantly influenced by P. From the previous analysis, it is clear that P can only affect the P error, i.e., the value of $E\left[(V)^{i+P}\right] - E[(V)^i]$, and cannot influence the numerical solution error. The purpose and significance of constructing the function $g_{\lambda',V}(h)$ is to find the optimal h value that minimizes the current numerical solution error. This optimal h value should only relate to the current V and N and is not influenced by P, and the numerical solution error will never be zero. Based on this, when N is even, directly calculating the optimal h value through the approach of Equation (39) is unreasonable. This is because the optimal h is directly related to the value of P, and when P changes, the corresponding optimal h value will change drastically. Consequently, this optimal h lacks stability, meaning that the method of determining the optimal h through the function $g_{\lambda',V}(h)$ is unstable and cannot be effectively applied in practice. Additionally, when the optimal h value is directly related to the value of P, any change in λ within the respective interval implies a change in P, meaning this optimal h cannot ensure the stability of the FFMT method's computational error, leading to a significant increase in error. Therefore, when N is even, Equation (39) should be further modified to make the calculated optimal h independent of P. Thus, when N is even, the function $g_{\lambda',V}(h)$ is modified as follows:

$$\begin{aligned} g_{\lambda',V}(h) &= \sum_{j=1}^{N} \frac{(-1)^{N-j} \cdot (\lambda' - N)}{\lambda' - j} \cdot \binom{\lambda'}{N} \cdot \binom{N}{j} \cdot E\left[(V)^j\right] \cdot h^{j-\lambda'} - E\left[(V)^i\right] \\ &= \mathcal{K}_1 \cdot \mathcal{U}_1 + \mathcal{K}_2 \cdot \mathcal{U}_2 + \cdots + \mathcal{K}_N \cdot \mathcal{U}_N \end{aligned} \tag{40}$$

The form of function $g_{\lambda',V}(h)$ proposed in Equation (40) effectively addresses the described issues, allowing for the calculation of the optimal h value that is not influenced by P. The modification to the form of Equation (40) is necessary because the first term ($\mathcal{K}_0\mathcal{U}_0$) of the original function $g_{\lambda',V}(h)$ does not contain significant integer-order moment information. Consequently, when λ varies within the corresponding integer interval, the first term $\mathcal{K}_0\mathcal{U}_0$ has minimal impact on the final computational result. Therefore, removing the first term to obtain the optimal h still ensures that the error of FFMT method remains within a low range. Additionally, after removing the first term, the curve shape of new function $g_{\lambda',V}(h)$ resembles that of the function when N is odd,

with only one minimum value. This similarity ensures that the optimal h value, unaffected by P, can be effectively obtained. The trend and sign change patterns of each term are consistent with those of the function $g_{\lambda',V}(h)$ when N is odd. The characteristics of the function $g_{\lambda',V}(h)$ in Equation (40) remain consistent with those when N is odd. Therefore, the method for calculating the corresponding optimal h value is the same as when N is odd. The corresponding expression is as follows:

$$\sum_{j=1}^{N} \frac{(-1)^{N-j} \cdot E\left[(V)^j\right]}{j! \cdot (N-j)!} \cdot h^j = 0 \tag{41}$$

Thus far, the analysis has focused on the characteristics of the function $g_{\lambda',V}(h)$ corresponding to different parity of N, as well as the existence and uniqueness of the corresponding optimal h. Furthermore, the validity of the method proposed in this paper for obtaining the optimal h value through the function $g_{\lambda',V}(h)$ has been demonstrated.

3.2.2 Calculation of the Optimal h

Based on the preceding argumentation, letting $Q_j = \frac{(-1)^{N-j}E\left[(V)^j\right]}{j!\cdot(N-j)!}$, the expression for calculating the optimal h as described above can be understood as solving the corresponding N-order univariate equation, as shown below:

$$\begin{cases} Q_1 h + Q_2 h^2 + \cdots + Q_N h^N - \dfrac{1}{N!} = 0 & for\ N\ is\ Odd \\ Q_1 h + Q_2 h^2 + \cdots + Q_N h^N = 0 & for\ N\ is\ Even \end{cases} \tag{42}$$

The methods for solving high-order univariate equations can be broadly classified into two categories: algebraic methods for analytical solutions and numerical solution methods. According to Galois Theory, for high-order univariate equations of degree 5 or higher, it is impossible to express solutions using a finite number of arithmetic operations and radicals. Given that N in Equation (42) can indeed be greater than 5, it is evident that using algebraic methods to obtain an analytical solution for Equation (42) is impractical. Considering that the h value calculated through Equation (42) does not require high precision—accuracy to four decimal places is sufficient to ensure the precision of the FFMT method's computational results—using numerical solution methods to solve Equation (42) is evidently more appropriate. And since Equation (42) contains only one unknown variable, applying relevant numerical solution techniques is straightforward. There are numerous well-known numerical methods for solving high-order univariate equations, including the bisection method, secant method, fixed-point iteration method, Newton-Raphson iteration method, and Taylor series expansion method. Considering that the optimal h does not require high precision to ensure the error level of the FFMT method, the more convenient and intuitive Taylor series expansion method is used here to solve Equation (42) to obtain the optimal h. For the sake of clarity, the function $q(h)$ corresponding to Equation (42) is given by the following expression:

$$q(h) = \begin{cases} Q_1 h + Q_2 h^2 + \cdots + Q_N h^N - \dfrac{1}{N!} & for\ N\ is\ Odd \\ Q_1 h + Q_2 h^2 + \cdots + Q_N h^N & for\ N\ is\ Even \end{cases} \tag{43}$$

Subsequently, a series of θ_i $(i = 0,1,2,\ldots,8,9)$ are provided, where except for $\theta_0 = 0.01$, the remaining θ_i values are given by $\theta_i = 0.1 \cdot i$. The Taylor series expansion method is then used to approximate the function $q(h)$ at different θ_i points, expanding it into the corresponding quadratic functions:

$$q(h) = q(\theta_i) + q^{(1)}(\theta_i) \cdot (h - \theta_i) + \frac{q^{(2)}(\theta_i)}{2} \cdot (h - \theta_i)^2 \tag{44}$$

Using Equation (44), the roots corresponding to $q(h) = 0$ for the Taylor series expansion at different θ_i points can be conveniently obtained. These roots are denoted by h_i^T, and the specific expression for h_i^T is given as follows:

$$h_i^T = \frac{-b_i \pm \sqrt{b_i^2 - 4 \cdot a_i \cdot c_i}}{2 \cdot a_i} \tag{45a}$$

$$a_i = \frac{q^{(2)}(\theta_i)}{2} \tag{45b}$$

$$b_i = q^{(1)}(\theta_i) - \theta_i \cdot q^{(2)}(\theta_i) \tag{45c}$$

$$c_i = q(\theta_i) - q^{(1)}(\theta_i) \cdot \theta_i + \frac{(\theta_i)^2 \cdot q^{(2)}(\theta_i)}{2} \tag{45d}$$

The method for obtaining h_i^T is based on the root-finding formula for a quadratic equation, where $q^{(n)}(\cdot)$ represents the n-th derivative of the function $q(h)$. When the difference between θ_i and h_i^T is minimized, then this h_i^T value is the optimal h sought. Given a function $y(h_i^T)$, denoted as $y(h_i^T) = |\theta_i - h_i^T|$, the optimal h value can be expressed by the following relationship:

$$Optimal\ h = argmin: y(h_i^T) = \left|\theta_i - h_i^T\right| \tag{46}$$

The h_i^T values in Equation (46) correspond to the real roots of Equation (44). If no real roots exist, the corresponding imaginary roots h_i^T values are not adopted. The advantage of using the above method to calculate the optimal h value lies in the elimination of the need for multiple iterations. Only 10 times calculations are required to obtain the corresponding optimal h value, significantly reducing the computational cost of the FFMT method in practical applications. On the other hand, for the Taylor series expansion of the function $q(h)$, in addition to being expanded into the form of a quadratic equation as in Equation (26), it can also be expanded into the form of a cubic Equation, denoted as $q(h) = q(\theta_i) + q^{(1)}(\theta_i) \cdot (h - \theta_i) + \frac{q^{(2)}(\theta_i)}{2} \cdot (h - \theta_i)^2 + \frac{q^{(3)}(\theta_i)}{6} \cdot (h - \theta_i)^3$. The cubic equation also has a root-finding formula, which allows for the roots to be obtained very conveniently. Increasing the number of terms in the Taylor expansion (like cubic Equation) can further improve the accuracy of the final optimal h value. It should be noted that the use of the Taylor expansion method to obtain the optimal h value here is due to its intuitive nature. However, in practical applications, more efficient solution methods may exist depending on the specific application environment and the nature of the random variables. Developing tailored solution methods for particular application settings can significantly enhance the computational efficiency of the FFMT method. Nevertheless, this aspect is not the focus of the present study, and therefore, it is not discussed further here.

At present, this study has provided the method for determining the values of parameters N and h. When applying the formula from Corollary 2.4 in practical scenarios, it is only necessary to determine the values of N and h using the described method. Then by combining these with the given integer-order moments of the corresponding random variable V and the values of the fractional order λ, the result $E\left[(V)^\lambda\right]$ can be calculated.

4. Numerical Experiments

In the numerical experiments part, it is assumed that the random variable V follows various types of distributions and use the FFMT method proposed in this paper to calculate the corresponding fractional moments, validating the FFMT method's effectiveness through experimental data. To present the validation results more clearly, fractional moments for different types of random variables V are calculated using either direct integration or analytical expressions. These results are considered the True Values and are compared with those obtained from the FFMT method. The accuracy of the FFMT method is assessed by measuring the error, defined as the difference between the FFMT-calculated results and the true values. Given that the Taylor expansion method, which is widely used in the engineering field for calculating fractional moments, also requires known integer moments (similar to the FFMT method), it serves as a suitable comparison. Consequently, the results include the error levels for fractional moments calculated using the Taylor expansion method under the same conditions. For consistency in comparison, when applying the Taylor expansion method, the number of expansion terms corresponds to the value of parameter N in the FFMT method.

(1) Truncated Normal Distribution

Assuming random variable V follows a truncated normal distribution. Employing the direct integration method computes the value of '$E[(V)^{\lambda}]$', which is regarded as the True Values. Specifying the distribution characteristics of V, denoted as '$V \sim TN(10,3)$', and truncation interval is $[0,30]$ Then as the fractional order λ varies, the computational results '$E[(V)^{\lambda}]$' obtained via FFMT method and Taylor expansion, respectively. The results are compared with the True Values and errors of the two methods are illustrated in the Figure 2. The figure demonstrates that the FFMT method exhibits minimal error fluctuations, consistently maintaining a very low level of error. This stability indicates that the FFMT method reliably produces highly accurate fractional order moment results, irrespective of the value of λ. In contrast, the Taylor expansion method also maintains high accuracy when λ is less than 3. However, when λ exceeds 4, the Taylor expansion method's error increases sharply with higher λ values, showing significant fluctuations. This suggests that the Taylor expansion method lacks the stability and accuracy of the FFMT method for higher-order moment calculations. This observation highlights the superiority of the FFMT method in handling high-order moments.

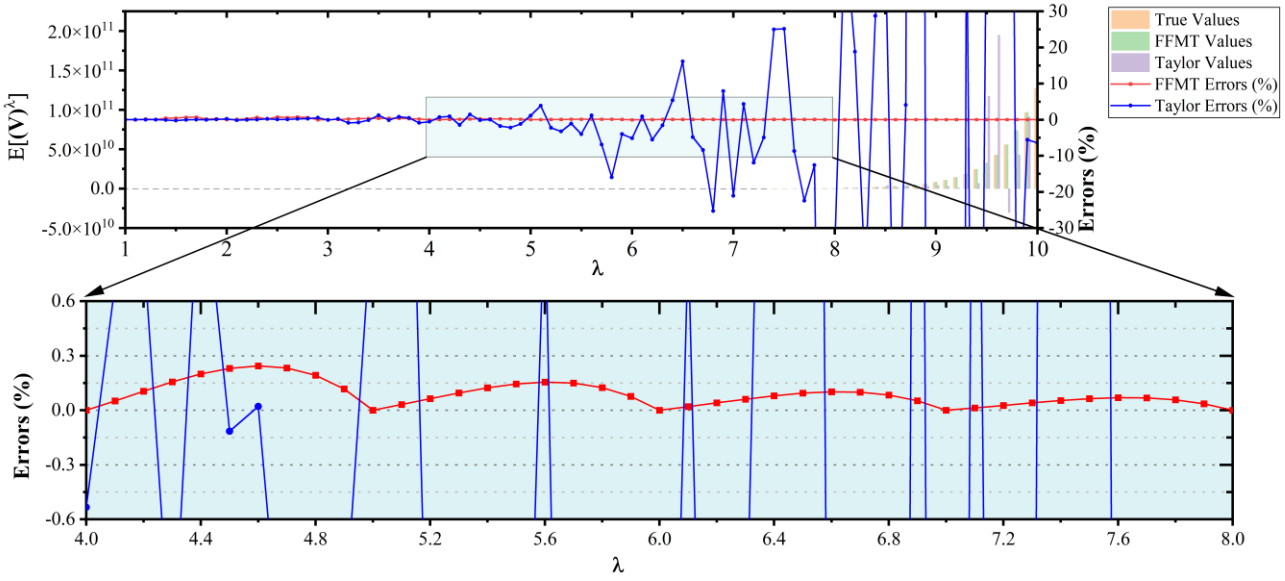

Fig 2. The errors of FFMT method and the Taylor expansion method compared to the True Values as λ varies, where the distribution is $V \sim TN(10,3)$ and truncation interval is $[0,30]$.

Figure 3 illustrates the error fluctuations of the FFMT method and the Taylor expansion method as λ varies, corresponding to changes in the standard deviation of a truncated normal distribution with a mean of 10 and a truncation range of $[0, 30]$. Figure 4 shows the error fluctuations of both methods as λ changes, corresponding to variations in the mean of a truncated normal distribution with a standard deviation of 5 and the same truncation range. The patterns observed in Figures 3 and 4 indicate that the overall error level of the FFMT method is directly related to the coefficient of variation of the random distribution. A higher coefficient of variation, indicating greater data dispersion, results in larger errors for the FFMT method. This is because higher data dispersion means the information contained in the same number of integer order moments is less effective at reflecting the corresponding fractional order moments. Thus, using these integer order moments to form a linear combination to obtain fractional order moments leads to increased errors. However, even when the coefficient of variation reaches 0.6, indicating significant data dispersion, the FFMT method's error remains controlled within 1%. Furthermore, regardless of changes in the coefficient of variation, the FFMT method maintains stable error levels as λ varies. In contrast, the Taylor expansion method's stability and accuracy are limited to lower fractional orders. As λ increases, the Taylor expansion method exhibits sharp error fluctuations and significant error increases. Therefore, the FFMT method demonstrates clear advantages over the Taylor expansion method for practical engineering applications.

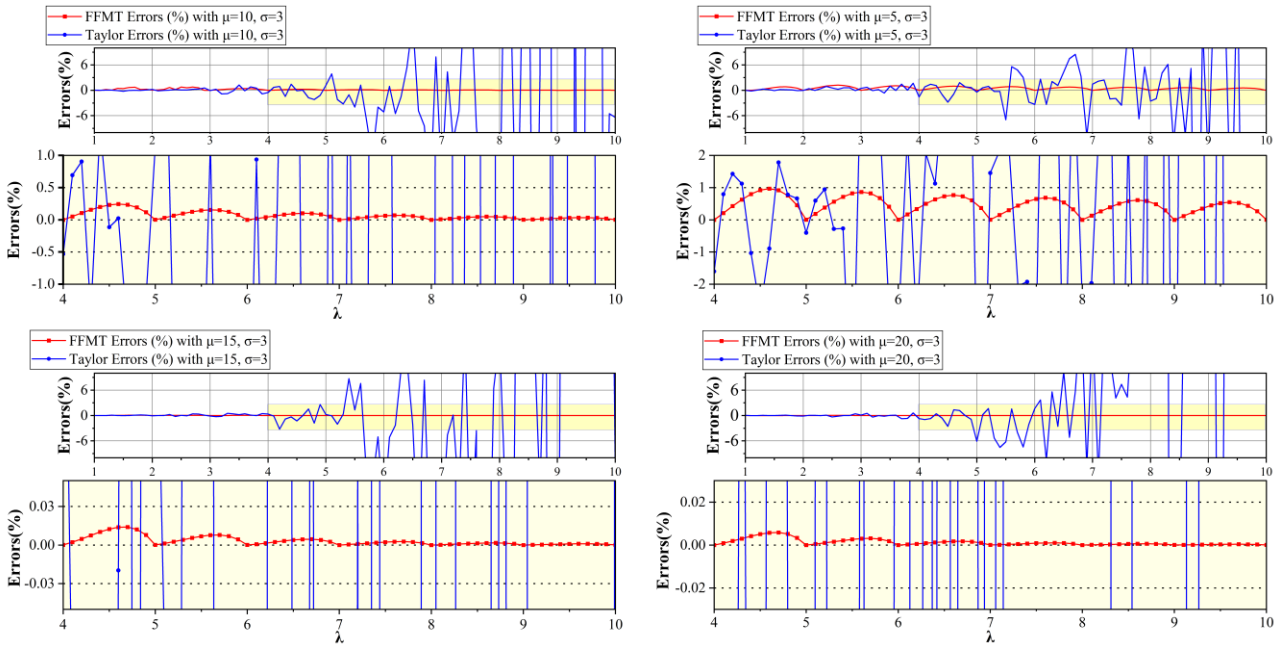

Fig 3. Errors of the FFMT method and the Taylor expansion method compared to the True Values as λ varies, considering different μ, denoted as $V \sim TN(\mu, 3)$, and truncation interval is $[0,30]$.

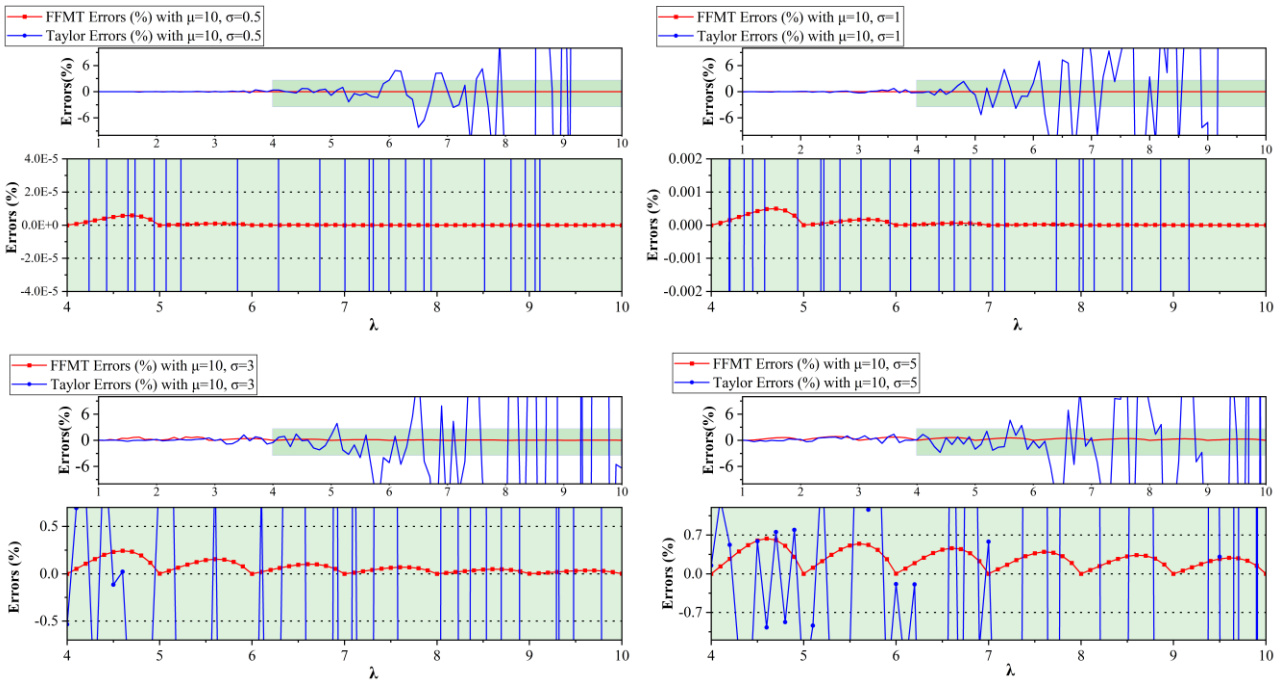

Fig 4. Errors of the FFMT method and the Taylor expansion method compared to the True Values as λ varies, considering different σ, denoted as $V \sim TN(10, \sigma)$, and truncation interval is $[0,30]$.

(2) Lognormal Distribution

Assuming the random variable V follows a lognormal distribution, denoted as $V \sim LN(1,0.5)$. The corresponding fractional moments of the specified order are computed directly using analytical expressions, which are regarded as the True Values. The expressions are presented as follows:

$$E\left[(V)^{\lambda}\right] = e^{\frac{1}{2}\cdot\lambda^2\cdot\sigma^2+\lambda\cdot\mu}$$

Figure 5 illustrates the results of $E[(V)^{\lambda}]$ calculated using the FFMT and Taylor expansion methods as the lognormal distribution varies with fractional order λ, along with the corresponding error levels compared to the True Values. From the Figure 5, it can be observed that although the Taylor expansion method no longer exhibits drastic errors when faced with the lognormal distribution, its error levels remain consistently high, averaging over 20% regardless of the variation in λ. In contrast, the FFMT method demonstrates excellent stability in error levels, coupled with high accuracy in results. The standard deviation of this lognormal distribution has already reached 50% of the mean, indicating a substantial degree of dispersion. However, even with such a large dispersion, the error in the results obtained using the FFMT method remains within 0.8% regardless of the variation in λ, demonstrating remarkably high accuracy.

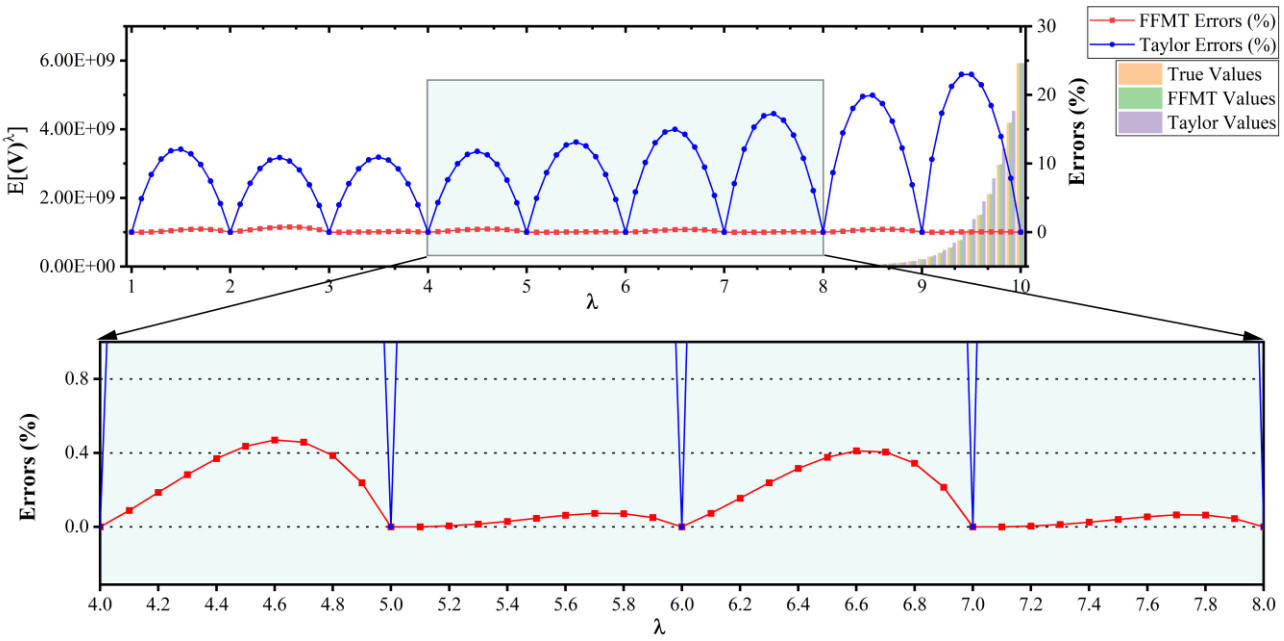

Fig 5. The errors of the FFMT method and the Taylor expansion method compared to the True Values as the distribution is $V \sim LN(1,0.5)$, while λ varies.

Figure 6 illustrates the error fluctuations of the FFMT method and the Taylor expansion method for lognormal distributions with varying means and standard deviations. The FFMT method consistently maintains a very low level of error regardless of changes in the mean and standard deviation of the log-normal distribution. Additionally, as the fractional order λ varies, the FFMT method's error remains stable, underscoring its robustness. In contrast, the Taylor expansion method exhibits significantly higher errors, which are not comparable to those of the FFMT method, demonstrating the superior accuracy of the FFMT method for lognormal distributions. Under the same mean or standard deviation conditions, the result precision of the FFMT method significantly exceeds that of the Taylor expansion method. As the mean of the log-normal distribution increases while the standard deviation remains constant, the error of the Taylor expansion method also increases. This occurs because the accuracy of the Taylor expansion method is influenced by the expansion point, typically the mean of the distribution in practical applications. Consequently, an increase in the mean results in greater error for the Taylor expansion method. The FFMT method effectively overcomes this limitation, maintaining a low and stable error level regardless of changes in the mean of the log-normal distribution. This stability highlights the FFMT method's reliability in practical engineering applications. As previously noted, increased dispersion of the random variable leads to higher errors for the FFMT method. However, even with greater dispersion, the FFMT method's error remains very low. This further demonstrates the FFMT method's advantage in accuracy.

On the other hand, comparing the error of the FFMT method for the lognormal distribution and the truncated normal distribution reveals that, within the same integer interval corresponding to a given λ, the error for the lognormal distribution is higher than that for the truncated normal distribution. This phenomenon occurs because the growth rate of the real-order moments for the lognormal distribution increases significantly more than that for the truncated normal distribution as the order λ increases. The FFMT method essentially involves linearly combining N integer-order moments with a proportion h to obtain the fractional-order moments within the corresponding interval. When the growth rate of the integer-order moments is higher, the growth rate of the

fractional-order moments within the integer interval is also greater. Therefore, using the same optimal h value within the same interval results in increased error for the FFMT method. This phenomenon also explains, in reverse, how different types of random distributions affect the error of the FFMT method. To address this, when the growth rate of the integer-order moments of a random variable is very high, it is necessary to consider variations in the optimal h value within the integer interval. Constructing an analytical expression that allows the optimal h value to change with the order λ can further improve the accuracy of the FFMT method. Given the focus of this study, a more in-depth discussion is not provided here.

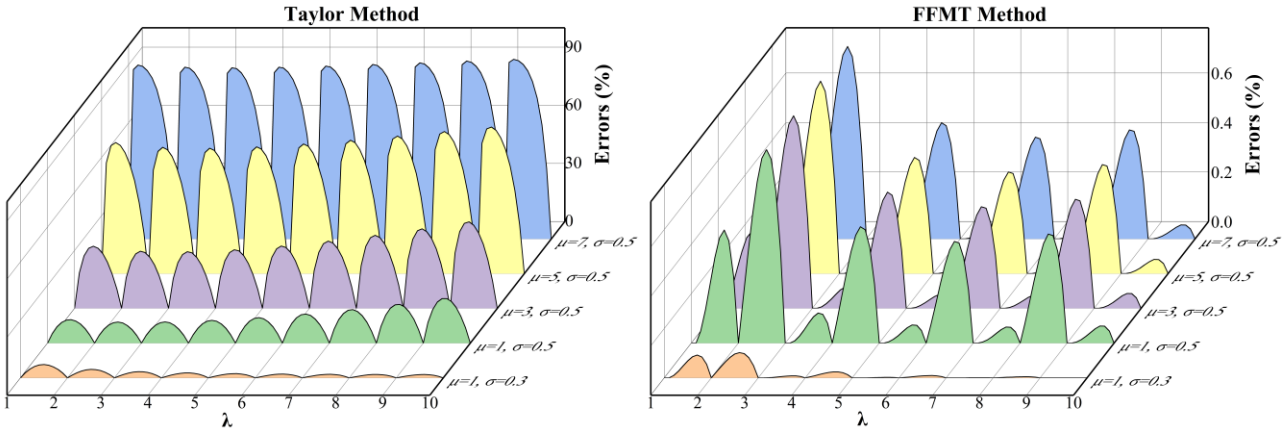

Fig 6. Errors of the FFMT method and the Taylor expansion method compared to True Values as λ varies, considering different σ and μ of the log-normal distribution.

(3) Gamma Distribution

As a typical example of a non-Gaussian distribution, the Gamma distribution is considered as the third case. Assuming the random variable V follows a Gamma distribution, denoted as '$V \sim \Gamma(k, \theta)$'. The True Values of different order moments are computed according to the following formula:

$$E\left[(V)^{\lambda}\right] = \theta^{\lambda} \frac{\Gamma(\mathrm{k}+\lambda)}{\Gamma(\mathrm{k})}$$

Figure 7 depicts the error fluctuations of the FFMT method and the Taylor expansion method as the parameters k and θ of the Gamma distribution vary. The FFMT method consistently maintains a very low and stable error level, regardless of the distribution characteristics of the random variable. In comparison, the Taylor expansion method exhibits errors that are several orders of magnitude higher than those of the FFMT method under identical distribution conditions. As the fractional order λ increases, the FFMT method's error fluctuations remain stable within a presentable range, avoiding increases with λ. In contrast, the Taylor expansion method's error fluctuations increase with λ, potentially causing negative impacts in practical engineering applications. This clearly demonstrates the FFMT method's superior output stability. When focusing on a specific integer interval of λ, the FFMT method's error increases as λ moves away from the interval boundary and decreases as λ approaches the boundary. This behavior is due to the FFMT method's reliance on linear combinations of integer order moments to obtain corresponding fractional order moments. As λ nears the boundary, the integer order moments more accurately represent the corresponding λ-order moment, resulting in smaller errors. Conversely, as λ moves away from the boundary, the same integer order moments are less effective, leading to increased errors. Nevertheless, within any integer interval, the FFMT method controls error fluctuations within a small range, ensuring highly accurate results.

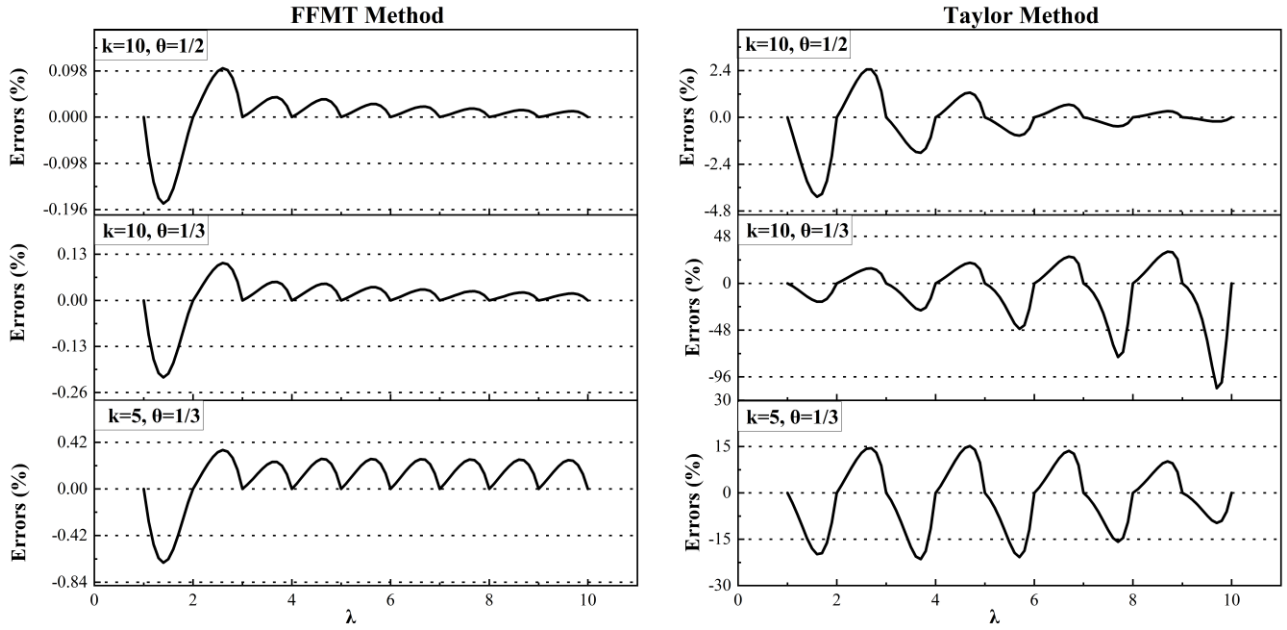

Fig 7. Errors of the FFMT method and Taylor expansion method compared to True Values as λ varies, considering different k and θ of gamma distribution.

The results demonstrate the feasibility and effectiveness of the FFMT method for calculating fractional order moments of random variables in the engineering field. The FFMT method exhibits two key advantages: accuracy and stability. The accuracy of the FFMT method ensures that highly precise fractional order moments can be obtained in practical applications, supporting the feasibility of subsequent research utilizing these moments. Stability refers to the method's ability to maintain errors within a very low and stable range, preventing abnormal fluctuations in the results. This stability ensures that the fractional order moments derived from the FFMT method will not cause aberrant outcomes in subsequent studies, thereby providing reliable data for further research.

(4) Real-world Application Case

To demonstrate the advantages of the FFMT method in practical engineering applications, a real-world example is added here for further analysis. In the stochastic traffic assignment problem, the BPR function is used to obtain the corresponding stochastic link travel time T_a [30], and its form is given as follows:

$$T_a = t_a^0 \cdot \left(1 + \beta \cdot \left(\frac{V_a}{C_a}\right)^{\lambda}\right)$$

where t_a^0 represents the free travel time of the link, C_a represents the link capacity, and β and λ are empirical parameters, which are positive real numbers. When the link capacity follows a certain random distribution and parameter λ takes a non-integer value, calculating the corresponding T_a leads to fractional moment problems. For the fractional moment problems in stochastic traffic assignment, the most used approach for solving these problems is the Taylor series expansion method [31]. However, in real-world networks, due to the large scale of the traffic network and the numerous links involved, the Taylor expansion method often cannot use adequate integer-order moments when considering computational costs, which results in inaccurate calculation outcomes. Based on this, a comparison between the FFMT method and the Taylor expansion method is conducted here, with both methods applied to stochastic traffic assignment to compare the traffic assignment results when

the network is in equilibrium. To ensure a fair comparison, both methods use $N = \lceil \lambda \rceil$ integer-order moments, allowing for a performance comparison while minimizing computational costs. The case uses the Nguyen and Dupuis network, which includes 13 nodes and 19 links, as illustrated in Figure 8.

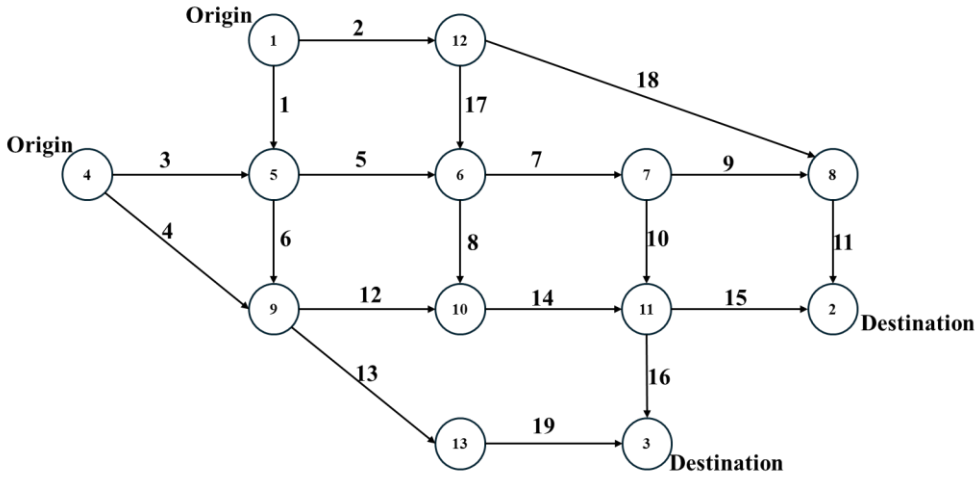

Fig 8. The Nguyen and Dupuis Network

Table 1

Random Link Capacity

Link Number	Mean	CV	Link Number	Mean	CV	Link Number	Mean	CV
1	2	0.3	8	2.7	0.2	15	3.4	0.1
2	2.1	0.3	9	2.8	0.2	16	3.5	0.1
3	2.2	0.3	10	2.9	0.2	17	3.6	0.1
4	2.3	0.3	11	3	0.2	18	3.7	0.1
5	2.4	0.3	12	3.1	0.2	19	3.8	0.1
6	2.5	0.3	13	3.2	0.1			
7	2.6	0.2	14	3.3	0.1			

Table 2

Path and link sequences

O-D pair	Path number	Link sequence
(1, 3)	1	1-6-13-19
	2	2-17-8-14-16
	3	2-17-7-10-16
	4	1-6-12-14-16
	5	1-5-7-10-16
	6	1-5-8-14-16

The free travel times for the links are set to 3. It is assumed that the link capacities follow a lognormal distribution, with the specific distribution parameters for each link shown in Table 1, where CV represents coefficient of variation. In this stochastic traffic assignment, (1, 3) is used as the O-D pair, with a total demand of 40. The link and path sequences in the network are provided in Table 2. The traffic assignment method follows the classical User Equilibrium (UE) principle [32], and the

corresponding assignment algorithm is the Method of Successive Averages (MSA) [30]. In the BPR function, parameter β is set to 0.15, and parameter λ is set to 5.5. After the network reaches equilibrium, the path flows and average travel times are shown in Table 3. Since the fractional moments of a lognormal distribution have an exact analytical solution, the results obtained using the analytical method are also included for comparison. Results of analytical method represent the fully accurate traffic assignment and are used to compare with the outcomes of the FFMT method and the Taylor expansion method. A comparison of the network assignment results shows that, after reaching equilibrium with the three different methods, the path flows obtained using the FFMT method are very close to those from the analytical method. The errors between the two are well within acceptable limits for practical applications of traffic assignment, indicating that the FFMT method ensures accuracy while controlling computational costs. However, when comparing the results from the Taylor expansion method, it is evident that there is a significant deviation from the analytical solution. Such a level of error is unacceptable in real-world applications. This demonstrates that the Taylor expansion method, when limited by the number of integer-order moments, leads to inaccurate results, and increasing the number of moments would require excessive computational resources. In contrast, the FFMT method manages to maintain accuracy while controlling computational costs, further highlighting its advantages in practical applications.

Table 3

Path flow and travel time values for the stochastic traffic assignment model at equilibrium using the Taylor expansion method, the analytical method, and the proposed method.

	Analytical Method		Proposed Method		Taylor Expansion Method	
	Path Flow	Path Time	Path Flow	Path Time	Path Flow	Path Time
Path 1	27.72	15.01219	27.76	15.00779	29.72	15.00021
Path 2	6.42	15.01089	6.38	15.01087	5.34	15.00259
Path 3	5.86	15.01089	5.86	15.01087	4.94	15.00259
Path 4	0	17.82058	0	17.81618	0	17.76587
Path 5	0	17.81223	0	17.8079	0	17.76126
Path 6	0	17.81223	0	17.80789	0	17.76126

5. Conclusion

To address the calculation of fractional order moments for positive random variables in the engineering field, this study derives an analytical solution for the fractional order moments by combining Laplace transforms and R-L type fractional derivatives. To enhance practical applicability, the study further develops a numerical solution using the principle of short memory principle and G-L type fractional derivatives based on the analytical solution. The stability and accuracy of the numerical solution are validated by demonstrating the existence of key parameters N and h, along with methods for determining their values, ensuring practical applicability. Data experiments validate that the FFMT method effectively addresses the calculation of fractional order moments for various random variables in engineering, thus facilitating research based on fractional order moments. Compared to traditional methods, such as the widely used Taylor expansion, the FFMT method demonstrates superior accuracy and stability, eliminating concerns regarding convergence. On the other hand, in terms of computational resource consumption, both the FFMT method and the Taylor

expansion method assume that the integer-order moments are known in practical applications. If obtaining the integer-order moments proves challenging, it can similarly affect the applicability of the FFMT method. However, given that the integer-order moments are known, the FFMT method requires fewer integer-order moments to ensure accurate results compared to the Taylor expansion method, thus significantly reducing computational resource demands in practical applications. The FFMT method, with its straightforward implementation, provides results with very low error levels and stable error fluctuations, benefiting practical engineering problems like probability density function reconstruction and distribution characteristic analysis.

There is still potential for further improvement of the FFMT method. Currently, the calculation of parameter h in the FFMT method employs the Taylor expansion method. However, many methods exist for solving univariate higher-order equations. Developing a more efficient method tailored to the specific characteristics of these equations when determining parameter h could further enhance the efficiency of the FFMT method in practical applications. Additionally, while using the same optimal h ensures accuracy as the fractional order λ varies within its integer interval, the optimal h value also exhibits a certain variation pattern with changes in λ. Identifying this pattern and formulating it as an analytical expression could further enhance the accuracy of the FFMT method significantly. Especially for different types of random distributions, the growth rate of their integer-order moments varies significantly. Consequently, as λ changes within its corresponding integer interval, the variation rate of the optimal h value also differs. If a specific mapping relationship between h and λ could be formulated based on the requirements of various practical distribution types, it would further optimize the accuracy of the results and greatly enhance the method's performance. This represents a significant direction for future research.

6. Statements and Declarations

This research did not receive any specific grant from funding agencies in the public, commercial, or not-for-profit sectors. The authors have no competing interests to declare that are relevant to the content of this article.

Appendix

A. Proof of Corollary 2.1

$$
\begin{aligned}
{}_{z}^{RL}D_{t}^{\lambda}f(t) &= \frac{1}{\Gamma(\zeta)}\frac{d^{k}}{dt^{k}}\int_{z}^{t}(t-\xi)^{\zeta-1}f(\xi)d\xi \\
&= \frac{1}{\Gamma(k-\lambda)}\frac{d^{k}}{dt^{k}}\left[\frac{(t-\lambda)^{k-\lambda}f(z)}{k-\lambda}+\int_{z}^{t}\frac{(t-\xi)^{k-\lambda}}{k-\lambda}f'(\xi)d\xi\right] \\
&= \frac{d^{k}}{dt^{k}}\left[\sum_{i=0}^{k-1}\frac{(t-\lambda)^{n+i-\lambda}f^{(i)}(z)}{\Gamma(\mathrm{n}+\mathrm{i}-\lambda+1)}+\frac{1}{\Gamma(2\mathrm{k}-\lambda)}\int_{z}^{t}(t-\xi)^{2k-\lambda-1}f^{(k)}(\xi)d\xi\right] \\
&= \sum_{i=0}^{k-1}\frac{(t-z)^{i-\lambda}f^{(i)}(z)}{\Gamma(\mathrm{i}-\lambda+1)}+\frac{1}{\Gamma(\mathrm{k}-\lambda)}\int_{z}^{t}(t-\xi)^{k-\lambda-1}f^{(k)}(\xi)d\xi \\
&= \sum_{i=0}^{k-1}\frac{(t-z)^{i-\alpha}f^{(i)}(z)}{\Gamma(\mathrm{i}-\lambda+1)}+{}_{z}^{C}D_{t}^{\lambda}f(t) \qquad (A.1)
\end{aligned}
$$

Form the equation $(A.1)$, when $z \to -\infty$, $\left(\sum_{i=0}^{k-1} \frac{(t-z)^{i-\alpha} f^{(i)}(z)}{\Gamma(i-\lambda+1)}\right)$ equals to 0, therefor the corollary 2.1 holds true.

B. Proof of Corollary 2.2

According to the definition of the R-L fractional integral:

$$
\begin{aligned}
{}^{R-L}_{z}I^{\lambda}_{t} f(t) &= \frac{1}{\Gamma(\lambda)} \int_{z}^{t} (t-\xi)^{\lambda-1} f(\xi) d\xi \\
&= \frac{1}{\Gamma(\lambda)} \int_{0}^{t-z} \xi^{\lambda-1} f(t-\xi) d\xi
\end{aligned} \tag{B.1}
$$

Given the conditions that $f(t) = e^{\varepsilon \cdot t}$, $a \to -\infty$, $\varepsilon > 0$, then:

$$
{}^{R-L}_{z}I^{\lambda}_{t} e^{\varepsilon \cdot t} = \frac{1}{\Gamma(\lambda)} \int_{0}^{\infty} \xi^{\lambda-1} e^{\varepsilon \cdot (t-\xi)} d\xi = \varepsilon^{-\lambda} e^{\varepsilon \cdot t} \tag{B.2}
$$

$$
{}^{C}_{z}D^{\lambda}_{t} e^{\varepsilon \cdot t} = D^{k} \lambda^{\lambda-k} e^{\varepsilon \cdot t} = \varepsilon^{\lambda} e^{\varepsilon \cdot t} \tag{B.3}
$$

This completes the proof of Corollary 2.2.

C. Proof of Corollary 2.3

Definition 2.5: Given an arbitrary real number z, $z \in \mathbb{R}$, and a non-integer number λ, $\lambda \in \mathbb{R}^{+}$ & $\lambda \notin \mathbb{N}$, $m-1 \leq \lambda < m \in \mathbb{Z}^{+}$. The left Grunwald-Letnikov fractional derivatives ${}^{GL}_{z}D^{\lambda}_{t} f$ of order λ of a function $f(t) \in C^{m}$ is also defined by[29]:

$$
\begin{aligned}
&{}^{GL}_{z}D^{\lambda}_{t} f(t) = \\
&\sum_{i=0}^{m} \frac{f^{(i)}(z)(t-z)^{-\lambda+i}}{\Gamma(-\lambda+i+1)} + \frac{1}{\Gamma(-\lambda+m+1)} \int_{z}^{t} (t-\xi)^{-\lambda+m} f^{(m+1)}(\xi) d\xi
\end{aligned} \tag{C.1}
$$

Let $k = \lceil \lambda \rceil$, $\zeta = k - \lambda$, $k-1 < \lambda < k$, the following relationship holds:

$$
\begin{aligned}
{}_{z}^{RL}D_t^{\lambda} f(t) &= \frac{d^k}{dt^k}\frac{1}{\Gamma(\zeta)}\int_z^t (t-\xi)^{\zeta-1} f(\xi)d\xi \\
&= \frac{d^k}{dt^k}\left[\sum_{i=0}^{m}\frac{f^{(i)}(z)(t-z)^{k-\lambda+i}}{\Gamma(k-\lambda+i+1)} + \frac{1}{\Gamma(k-\lambda+m+1)}\int_z^t (t-\xi)^{k-\lambda+m} f^{m+1}(\xi)d\xi\right] \\
&= \sum_{i=0}^{m}\frac{f^{(i)}(z)\frac{d^k}{dt^k}(t-z)^{k-\lambda+i}}{\Gamma(k-\lambda+i+1)} + \frac{1}{\Gamma(k-\lambda+m+1)}\int_z^t \frac{d^k}{dt^k}\left[(t-\xi)^{k-\lambda+m}\right] f^{m+1}(\xi)d\xi \\
&= \sum_{i=0}^{m}\frac{f^{(i)}(z)(k-\lambda+i)\frac{d^{k-1}}{dt^{k-1}}(t-z)^{k-\lambda+i-1}}{(k-\lambda+i)\Gamma(k-\lambda+i)} + \\
&\frac{1}{(k-\lambda+m)\Gamma(k-\lambda+m)}\int_z^t (k-\lambda+m)\frac{d^{k-1}}{dt^{k-1}}\left[(t-\xi)^{k-\lambda+m-1}\right] f^{m+1}(\xi)d\xi \\
&= \sum_{i=0}^{m}\frac{f^{(i)}(z)\frac{d^{k-1}}{dt^{k-1}}(t-z)^{k-\lambda+i-1}}{\Gamma(k-\lambda+i)} + \frac{1}{\Gamma(k-\lambda+m)}\int_z^t \frac{d^{k-1}}{dt^{k-1}}\left[(t-\xi)^{k-\lambda+m-1}\right] f^{m+1}(\xi)d\xi \\
&= \cdots \\
&= \sum_{i=0}^{m}\frac{f^{(i)}(z)(t-z)^{k-\lambda+i-k}}{\Gamma(k-\lambda+i+1-k)} + \frac{1}{\Gamma(k-\lambda+m+1-k)}\int_z^t \left[(t-\xi)^{k-\lambda+m-k}\right] f^{m+1}(\xi)d\xi \\
&= {}_{z}^{GL}D_t^{\lambda} f(t) \qquad (C.2)
\end{aligned}
$$

This completes the proof of the corollary 2.3.

D. Proof of Corollary 2.4

For sufficiently small h, according to the definition of integer-order derivatives, the following expansion can be obtained:

$$
f^{(n)}(t) = \frac{(-1)^0 C_n^0 f(t-0h) + (-1)^1 C_n^1 f(t-1h) + (-1)^2 C_n^2 f(t-2h) + \cdots + (-1)^n C_n^n f(t-nh)}{h^n} \qquad (D.1)
$$

Performing the inverse transformation on Equation (D.1) yields:

$$
\begin{aligned}
f(t-nh) &= h^0(-1)^0 C_n^0 f^{(0)}(t) + h^1(-1)^1 C_n^1 f^{(1)}(t) + h^2(-1)^2 C_n^2 f^{(2)}(t) + \\
&\quad \ldots + h^n(-1)^n C_n^n f^{(n)}(t) \\
&= \sum_{i=0}^{n} h^i(-1)^i C_n^i f^{(j)}(t) \qquad (D.2)
\end{aligned}
$$

According to Definition 2.5, combined with Equations (13) and (D.2), the following relationship can be further derived:

$$
\begin{aligned}
&E\left[(V)^{\lambda}\right] \\
&= {}_{s-L}^{GL}D_s^{\alpha}\left(\mathcal{L}\{p(V)\}(s)\right)\Big|_{s=0} \\
&= \sum_{i=0}^{N}(-1)^i\binom{\lambda}{i}\sum_{j=0}^{i}(-1)^j\binom{i}{j}h^{j-\lambda}\frac{d^j}{ds^j}\left(\mathcal{L}\{p(V)\}(s)\right)\Big|_{s=0} \\
&= \sum_{i=0}^{N}\sum_{j=0}^{i}(-1)^{i-j}\binom{\lambda}{i}\binom{i}{j}h^{j-\lambda}\frac{d^j}{ds^j}\left(\mathcal{L}\{p(V)\}(s)\right)\Big|_{s=0} \\
&= \sum_{j=0}^{N}\sum_{i=j}^{N}(-1)^{i-j}\binom{\lambda}{i}\binom{i}{j}h^{j-\lambda}\frac{d^j}{ds^j}\left(\mathcal{L}\{p(V)\}(s)\right)\Big|_{s=0} \\
&= \sum_{j=0}^{N}\frac{(-1)^{N-j}(\lambda-N)}{\lambda-j}\binom{\lambda}{N}\binom{N}{j}h^{j-\lambda}\frac{d^j}{ds^j}\left(\mathcal{L}\{p(V)\}(s)\right)\Big|_{s=0} \\
&= \sum_{j=0}^{N}\frac{(-1)^{N-j}(\lambda-N)}{\lambda-j}\binom{\lambda}{N}\binom{N}{j}h^{j-\lambda}E\left[(V)^j\right] \qquad (D.3)
\end{aligned}
$$

This completes the proof of Corollary 2.4.

E. Proof of Corollary 2.5

Given $|f(t)| \le M$, $a + L < b$, L is the memory length, and $\Delta(t)$ denotes the error, then the following inequality holds:

$$
\begin{aligned}
&\Delta(t) = \left|{}_{-\infty}^{GL}D_t^{\lambda}f(t) - {}_{t-L}^{GL}D_t^{\lambda}f(t)\right| = \\
&\left|\frac{1}{\Gamma(-\lambda)}\right|\left|\int_{-\infty}^{t}\frac{f(\xi)}{(t-\xi)^{\lambda+1}}d\xi - \int_{t-L}^{t}\frac{f(\xi)}{(t-\xi)^{\lambda+1}}d\xi\right| \\
&\le \left|\frac{1}{\Gamma(-\lambda)}\right|\left|\int_{-\infty}^{t}\frac{f(\xi)}{(t-\xi)^{\lambda+1}}d\xi - \int_{-\infty}^{t-L}\frac{f(\xi)}{(t-\xi)^{\lambda+1}}d\xi\right| \\
&= \left|\frac{1}{\Gamma(-\lambda)}\right|\left|\int_{t-L}^{t}\frac{f(\xi)}{(t-\xi)^{\lambda+1}}d\xi\right| \\
&\le \left|\frac{1}{\Gamma(-\lambda)}\right|\left|\int_{t-L}^{t}\frac{M}{(t-\xi)^{\lambda+1}}d\xi\right| \\
&= \frac{ML^{-\lambda}}{|\Gamma(1-\lambda)|} \qquad (E.1)
\end{aligned}
$$

Given a required accuracy ε, ε can impose a direct impact on the memory length, if $\Delta(t) \le \varepsilon$, then ε further determine the memory length L:

$$
L \ge \left(\frac{M}{\varepsilon\,|\Gamma(1-\lambda)|}\right)^{\frac{1}{\lambda}} \qquad (E.2)
$$

Reference

[1] C. Luo, S.-P. Zhu, B. Keshtegar, W. Macek, R. Branco, and D. Meng, "Active Kriging-based conjugate first-order reliability method for highly efficient structural reliability analysis using

resample strategy," *Computer Methods in Applied Mechanics and Engineering,* vol. 423, p. 116863, 2024/04/01/ 2024, doi: https://doi.org/10.1016/j.cma.2024.116863.

[2] D. Meng, S. Yang, H. Yang, A. M. P. De Jesus, J. Correia, and S.-P. Zhu, "Intelligent-inspired framework for fatigue reliability evaluation of offshore wind turbine support structures under hybrid uncertainty," *Ocean Engineering,* vol. 307, p. 118213, 2024/09/01/ 2024, doi: https://doi.org/10.1016/j.oceaneng.2024.118213.

[3] S. Yang, D. Meng, H. Wang, and C. Yang, "A novel learning function for adaptive surrogate-model-based reliability evaluation," *Philosophical Transactions of the Royal Society A: Mathematical, Physical and Engineering Sciences,* vol. 382, no. 2264, p. 20220395, 2024, doi: doi:10.1098/rsta.2022.0395.

[4] M. Matsui, Z. Pawlas, and x11b, "Fractional absolute moments of heavy tailed distributions," *Brazilian Journal of Probability and Statistics,* vol. 30, no. 2, pp. 272-298, 2016. [Online]. Available: http://www.jstor.org/stable/24913854.

[5] S. R. Durrans, "Distributions of fractional order statistics in hydrology," *Water Resources Research,* vol. 28, no. 6, pp. 1649-1655, 1992, doi: https://doi.org/10.1029/92WR00554.

[6] T. Lefebvre, "On Moment Estimation From Polynomial Chaos Expansion Models," *IEEE Control Systems Letters,* vol. 5, no. 5, pp. 1519-1524, 2021, doi: 10.1109/LCSYS.2020.3040851.

[7] L. Novák, M. Valdebenito, and M. Faes, *Fractional moment estimation from Polynomial Chaos Expansions*. 2024.

[8] G. Laue, "Remarks on the relation between fractional moments and fractional derivatives of characteristic functions," *Journal of Applied Probability,* vol. 17, no. 2, pp. 456-466, 1980.

[9] I. Dremin, "Fractional moments of distributions," *JETP Letters,* vol. 59, no. 9, pp. 585-588, 1994.

[10] T. Sandev, R. Metzler, and Ž. Tomovski, "Fractional diffusion equation with a generalized Riemann–Liouville time fractional derivative," *Journal of physics A: mathematical and theoretical,* vol. 44, no. 25, p. 255203, 2011.

[11] G. Cottone and M. Di Paola, "On the use of fractional calculus for the probabilistic characterization of random variables," *Probabilistic Engineering Mechanics,* vol. 24, no. 3, pp. 321-330, 2009.

[12] H. Gzyl and A. Tagliani, "Hausdorff moment problem and fractional moments," *Applied Mathematics and Computation,* vol. 216, no. 11, pp. 3319-3328, 2010.

[13] K. H. Biyari and W. C. Lindsey, "Statistical distributions of Hermitian quadratic forms in complex Gaussian variables," *IEEE transactions on information theory,* vol. 39, no. 3, pp. 1076-1082, 1993.

[14] R. Benouini, I. Batioua, K. Zenkouar, A. Zahi, S. Najah, and H. Qjidaa, "Fractional-order orthogonal Chebyshev moments and moment invariants for image representation and pattern recognition," *Pattern Recognition,* vol. 86, pp. 332-343, 2019.

[15] A. Tagliani, "Hausdorff moment problem and fractional moments: A simplified procedure," *Applied mathematics and computation,* vol. 218, no. 8, pp. 4423-4432, 2011.

[16] M. Haas and C. Pigorsch, "Financial Economics, Fat-Tailed Distributions," *Encyclopedia of Complexity and Systems Science,* vol. 4, no. 1, pp. 3404-3435, 2009.

[17] G. Consigli, "Tail estimation and mean–VaR portfolio selection in markets subject to financial instability," *Journal of Banking & Finance,* vol. 26, no. 7, pp. 1355-1382, 2002.

[18] H. Zhao, S. Li, and C. Zhu, "Uncertainty analysis of rock tunnel based on fractional moment and dimensional reduction method," *International Journal of Rock Mechanics and Mining Sciences,* vol. 139, p. 104656, 2021.

[19] C. Feng, M. A. Valdebenito, M. Chwała, K. Liao, M. Broggi, and M. Beer, "Efficient slope reliability analysis under soil spatial variability using maximum entropy distribution with fractional moments," *Journal of Rock Mechanics and Geotechnical Engineering,* vol. 16, no. 4, pp. 1140-1152, 2024.

[20] A. Gelman, "Method of moments using Monte Carlo simulation," *Journal of Computational and Graphical Statistics,* vol. 4, no. 1, pp. 36-54, 1995.

[21] J. E. Gentle, "Monte carlo methods," *Random number generation and Monte Carlo methods,* pp. 229-281, 2003.

[22] J. Xu and C. Dang, "A novel fractional moments-based maximum entropy method for high-dimensional reliability analysis," *Applied Mathematical Modelling,* vol. 75, pp. 749-768, 2019.

[23] H. C. Frey and D. E. Burmaster, "Methods for characterizing variability and uncertainty: comparison of bootstrap simulation and likelihood-based approaches," *Risk analysis,* vol. 19, no. 1, pp. 109-130, 1999.

[24] F. Salvat, J. M. Fernández-Varea, J. Sempau, and J. Mazurier, "Practical aspects of Monte Carlo simulation of charged particle transport: Mixed algorithms and variance reduction techniques," *Radiation and environmental biophysics,* vol. 38, no. 1, pp. 15-22, 1999.

[25] X. Zhang and M. D. Pandey, "Structural reliability analysis based on the concepts of entropy, fractional moment and dimensional reduction method," *Structural Safety,* vol. 43, pp. 28-40, 2013.

[26] R. Remmert, "The Gamma Function," in *Classical Topics in Complex Function Theory*, R. Remmert Ed. New York, NY: Springer New York, 1998, pp. 33-72.

[27] T. F. NONNENMACHER and R. METZLER, "ON THE RIEMANN-LIOUVILLE FRACTIONAL CALCULUS AND SOME RECENT APPLICATIONS," *Fractals,* vol. 03, no. 03, pp. 557-566, 1995, doi: 10.1142/s0218348x95000497.

[28] Y. Luchko, *Fractional Integrals and Derivatives: "True" versus "False"*. 2021.

[29] I. Podlubny, *Fractional Differential Equations: An Introduction to Fractional Derivatives, Fractional Differential Equations, to Methods of Their Solution and Some of Their Applications*. Elsevier Science, 1998.

[30] Y. Sheffi, *Urban Transportation Networks: Equilibrium Analysis With Mathematical Programming Methods*. 1984.

[31] H. Shao, W. H. K. Lam, and M. L. Tam, "A Reliability-Based Stochastic Traffic Assignment Model for Network with Multiple User Classes under Uncertainty in Demand," *Networks and Spatial Economics,* vol. 6, no. 3, pp. 173-204, 2006/09/01 2006, doi: 10.1007/s11067-006-9279-6.

[32] J. G. WARDROP, "ROAD PAPER. SOME THEORETICAL ASPECTS OF ROAD TRAFFIC RESEARCH," *Proceedings of the Institution of Civil Engineers,* vol. 1, no. 3, pp. 325-362, 1952, doi: 10.1680/ipeds.1952.11259.